Invited Review Article for Nature Reviews Earth & Environment

Revised 28 September 2023

Short- and long-term variability of the Antarctic and Greenland ice sheets

Edward Hanna[1+], Dániel Topál[2,3], Jason E. Box[4], Sammie Buzzard[5], Frazer D. W. Christie[6], Christine Hvidberg[7], Mathieu Morlighem[8], Laura De Santis[9], Alessandro Silvano[10], Florence Colleoni[9], Ingo Sasgen[11], Alison F Banwell[12], Michiel R. van den Broeke[13], Robert DeConto[14], Jan De Rydt[15], Heiko Goelzer[16], Alexandra Gossart[17], G. Hilmar Gudmundsson[15], Katrin Lindbäck[18,19], Bertie Miles[20], Ruth Mottram[21], Frank Pattyn[22], Ronja Reese[15], Eric Rignot[23], Aakriti Srivastava[24], Sainan Sun[15], Justin Toller[25], Peter A. Tuckett[26], Lizz Ultee[27]

[1]*Department of Geography, University of Lincoln, Lincoln, UK*

[2]*Institute for Geological and Geochemical Research, Research Centre for Astronomy and Earth Sciences (MTA-Centre of Excellence), ELKH, Budapest, Hungary*

[3]*Earth and Life Institute, Université catholique de Louvain, Louvain-la-Neuve, Belgium*

[4]*Geological Survey of Denmark & Greenland, Copenhagen, Denmark*

[5]*School of Earth & Environmental Sciences, University of Cardiff, Cardiff, UK*

[6]*Scott Polar Research Institute, University of Cambridge, Cambridge, UK*

[7]*Niels Bohr Institute, University of Copenhagen, Copenhagen, Denmark*

[8]*Department of Earth Sciences, Dartmouth College, Hanover, NH, USA*

[9]*Section of Geophysics, National Institute of Oceanography and Applied Geophysics, Trieste, Italy*

[10]*Ocean and Earth Science, National Oceanography Centre, University of Southampton, Southampton, UK*

[11]*Alfred Wegener Institute, Bremerhaven, Germany*

[12]*Cooperative Institute for Research in Environmental Sciences (CIRES), University of Colorado Boulder, Boulder, CO, USA*

[13]*Institute for Marine and Atmospheric research Utrecht, Utrecht University, Utrecht, The Netherlands*
[14]*Department of Earth, Geographic, and Climate Sciences, College of Natural Sciences, University of Massachusetts Amherst, Amherst, MA, USA*
[15]*Department of Geography and Environmental Sciences, Northumbria University, Newcastle, UK*
[16]*Norce Norwegian Research Centre, Bjerknes Centre for Climate Research, Bergen, Norway*
[17]*Antarctic Research Centre | Te Puna Pātiotio, Victoria University of Wellington | Te Herenga Waka, Wellington| Te Whanganui –a-Tara , New Zealand | Aotearoa*
[18]*Division of Research and Educational Support, Mid Sweden University, Östersund, Sweden*
[19]*Norwegian Polar Institute, Tromsø, Norway*
[20]*School of Geosciences, University of Edinburgh, Edinburgh, UK*
[21]*Danish Meteorological Institute, Copenhagen, Denmark*
[22]*Departement of Geosciences, Environnement,* Society, *Université Libre de Bruxelles, Brussels, Belgium*
[23]*Department of Earth System Science, University of California Irvine, Irvine, CA, USA*
[24]*Department of Earth Science, Barkatullah University, Bhopal, India*
[25]*Department of Geological Sciences and Engineering, University of Nevada, Reno, NV, USA*
[26]*Department of Geography, University of Sheffield, Sheffield, UK*
[27]*Department of Earth and Climate Sciences, Middlebury College, Vermont, USA*
[+]*e-mail: ehanna@lincoln.ac.uk*

Abstract. Antarctic and Greenland Ice Sheet variability occurs on various timescales and is important for projections of sea-level rise; however, significant uncertainties remain concerning ice-sheet mass changes during and beyond the rest of this century. In this review we explore the degree to which short-term fluctuations and extreme glaciological events over the last three decades reflect the ice sheets' longer-term evolution and response to ongoing climate change. Short-term (decadal or shorter) variations in atmospheric or oceanic conditions can trigger amplifying feedbacks that ultimately increase ice-sheet sensitivity to climate change. Variability in ocean- and atmosphere-induced melting has the potential to trigger ice thinning, retreat and/or collapse of ice shelves, grounding-line retreat and ice-flow acceleration. Greatly contrasting Greenland melt anomalies since 2012, for example, highlight the role of increased interannual climate variability on extreme glaciological events and ice-sheet evolution. Failing to adequately account for such seasonal- to decadal-scale variability can result in biased projections of multi-decadal ice mass-loss. Future research priorities therefore include fully realising advances in Earth observation, climate and ocean datasets and models, and developing and implementing more sophisticated ice-sheet models that are constrained directly by observational records and can capture ice-dynamical changes across a wide range of timescales.

Introduction

The Antarctic Ice Sheet (AIS) and Greenland Ice Sheet (GrIS) have together overtaken the mountain glaciers as the main cryospheric contributor[1] to accelerating global mean sea-level rise, contributing 382(±42) Gt yr^{-1} (~1.1 mm yr^{-1}) of sea-level, equivalent or almost one third of total sea-level rise) from 2002 to 2022 (Figure 1). Almost two-thirds of this estimated mass loss, 255(±19) Gt yr^{-1}, was from the GrIS, which partly reflects warmer summer conditions for much of Greenland compared with Antarctica; however, for both ice sheets considerable year-to-year mass variability is superimposed upon the highly significant downward trends (Figure 1). The main mass-loss contributions came from the southern half of the GrIS and the low-elevation areas of the West AIS, while the much smaller Antarctic Peninsula region underwent only relatively small mass losses and the East AIS slightly gained mass during the 21-year period (Figure 1).

The period since around 2000 has seen well-documented changes in the ice sheets[2], with the dramatic breakup of several Antarctic ice shelves (for example in 1995, 2002 and 2008) and a selection of major GrIS surface melt events (for example in 2012, 2019 and 2022) perhaps being the most iconic. Some of these short-term events (e.g. the major GrIS melt episodes of July 2012 and July/August 2019) can easily be identified as distinct downward anomalies in the GrIS mass fluctuations where relatively short-term events (a few days to a few weeks) meant that those year's mass losses were approximately double those of surrounding years (Figure 1b). However, it remains unclear how indicative such short-term extreme events are of longer-term change and what the relative role of system-intrinsic variability (sub-daily to decadal timescale variations in atmosphere and ocean circulation and ice dynamics) versus longer-term external forcing (especially climate change over some decades or centuries) is: in other words, the importance of ice-sheet 'weather' versus 'climate'.

As a result of this long- vs. short- term variability, amidst various sources of uncertainty[1], computer-model projections of future ice-sheet mass change that crucially underpin sea-level projections are uncertain, with crucial ramifications for climate adaptation (for example coastal protection strategies) and implications for mitigation. This uncertainty is exacerbated because ice-sheet model projections are often forced by average conditions excluding extremes or variances.

In this review, we apply a multi-disciplinary perspective to the latest evidence from observations and models of ice-sheet change to help overcome this impasse. We first outline the key drivers (atmosphere and ocean) and hydrological processes that are involved in ice-sheet change. Next, we explore short- and long- term changes in the AIS and GrIS, and the interrelations between these timescales that can yield key insights into ice-sheet sensitivity and response to ongoing climate warming. The final part of the paper synthesises our findings and makes priority research recommendations for the next five years to the international research community, funding agencies and policymakers.

Drivers and processes of ice-sheet mass change

Ice-sheet mass budget is a function of surface mass balance (predominantly net snow accumulation minus the runoff of surface meltwater), basal mass balance (net mass change due to accumulation and melting at the base of an ice sheet or ice shelf), and dynamics (ice flow and calving) (Figure 2). Ice-sheet mass change is driven by various processes (Figure 2), including variations in atmospheric and oceanic forcing, and hydrology, each of which we discuss in the following sections. In addition, we consider the effect of sea-ice on ice-sheet change and introduce two potential ice-sheet instabilities.

Atmospheric forcing

The atmosphere interacts with the mass balance of ice sheets on a wide range of spatial (sub-metre to hundreds of km) and temporal (sub-minute to decadal) scales (Figure 2). Atmospheric circulation impacts ice sheets primarily via its direct influence on accumulation/ablation by regulating snow and rainfall and the surface energy balance (the net amount of energy from radiation and heat fluxes at the ice-sheet surface that goes into controlling surface temperature changes, melt and surface mass losses). Along ice-sheet margins, daily to weekly timescales and tens to hundreds of kilometre spatial scales dominate. Atmospheric events such as foehn and katabatic winds (relatively warm and cold downslope mountain winds, respectively) can also impact the snow/ice accumulation and surface melt rate[3].

Snow accumulation across both ice sheets decreases from the margin, where it can locally reach values well above 1 m per year water equivalent (WE), towards the elevated interior ice sheet, where colder and drier conditions prevail. In the high interior, where accumulation rates are below 10 cm per year WE (polar deserts), a marked fraction of precipitation is caused by 'diamond dust'. This phenomenon results from radiative cooling and quasi-steady snow crystal formation when the lower atmosphere saturates accordingly[4,5], which climate models struggle to represent well[6]. In the south-eastern GrIS and over the Antarctic Peninsula, topographic lifting of relatively warm and moist air masses enhance snowfall amounts[7,8]. Atmospheric rivers - episodic narrow bands of enhanced moisture transport - enhance downwelling longwave radiation and cause high-melt episodes that are often contemporaneous with large amounts of snowfall[9–11]. While snowfall from large synoptic-scale systems is relatively spatially homogeneous, in-air sublimation in the dry polar atmosphere[12] and sublimation and erosion by near-surface (katabatic and foehn) winds[13,14] can also introduce significant small-scale spatial variability that complicates accumulation studies from in-situ observations using stakes or firn cores[8].

An observed increase towards a more negative North Atlantic Oscillation (NAO) in summer, with accompanying anticyclonic circulation anomalies ("blocking") over the western GrIS, since the 1990s[15] has enhanced surface melt and runoff by regulating complex interactions between components of the radiation budget[16,17] and thus the surface mass balance. Descending air inside the anticyclone together with low-level warm advection accompany extreme melt episodes[18], with part of the related circulation anomalies linked to low-frequency tropical Pacific sea-surface temperature variability[19]. Similarly, shallow surface-based temperature inversions[20] and accompanying cloud-radiative anomalies[21,22] also have a key role (especially in increased melting recorded in northern Greenland) but remain poorly constrained in climate models.

Although most of the AIS's current mass loss occurs via ice-shelf basal melting and iceberg calving, its interannual surface mass balance variability is dominated by atmospheric processes[23]. A combination of stratospheric ozone depletion, greenhouse gas emissions and multidecadal Pacific/Atlantic sea-surface temperature variabilities has been suggested to drive a trend towards a more positive Southern Annular Mode (i.e. stronger westerly winds which contract towards Antarctica) since the 1950s[24], which has in turn been linked to Antarctic ice-shelf basal melting[25] enabled by enhanced circumpolar deep water upwelling[26] and AIS precipitation changes[27]. However, it is notable that since 1980 Antarctic ice shelves experienced only minor changes in surface melt[28]. The top 10% of daily precipitation totals contribute around half of the total annual precipitation events and therefore dominate SMB over much of the AIS, especially in coastal areas including over the ice shelves[29].

Buried snow slowly (decades to millennia) transforms into ice in the up to 120 m thick firn layer[30,31]. The firn layer acts as a low-pass filter between short-term atmospheric variability in snowfall (replenishing firn pore space) and melt (destroying it), and thus acts to modulate the response of the ice sheet to atmospheric forcing. Refreezing is also critical because this caps the firn and increases runoff. Over the GrIS, for example, firn layer saturation translates into the expansion of the runoff zone which can ultimately lead to accelerated mass loss. These quasi-irreversible changes in the firn layer provide a useful baseline for helping to distinguish ice-sheet weather from climate.

Oceanic forcing

Oceanic forcing drives ice-sheet mass loss by melting marine-terminating glaciers and ice shelves (Figure 2). In Greenland, most of the glaciers that reach the coast terminate into fjords as cliff-like vertical ice fronts. There, submarine melting is regulated by turbulent fluxes that transport oceanic heat toward the ice front. These turbulent fluxes are controlled by the ocean temperatures in the fjords and plumes that develop adjacent to the ice front[32]. Relatively high oceanic temperatures are associated with inflow of Atlantic waters into the fjords at depth[33], while plumes originate from subglacial melt-water discharge that is ultimately driven by surface melting and subsequent runoff (which, in turn, is closely linked to atmospheric forcing[32]). Submarine melting might also cause the indirect retreat of marine-terminating glaciers by enhancing iceberg discharge[34-36]. Collectively, oceanic forcing has been implicated in the multidecadal retreat and thinning of tens of coastal glaciers around Greenland since at least the early 1990s, as well as decadal oscillations in their frontal position and thickness[32,37].

Unlike the GrIS, approximately 75% of the AIS' periphery is surrounded by floating ice shelves[38]. Since the beginning of routine satellite observations in the early 1990s, most of the multidecadal mass loss of the AIS has occurred in regions exhibiting strong basal melting, retreat, and thinning of ice shelves[23,39-41], implicating oceanic forcing as a key driver. Interannual to multi-decadal acceleration, thinning and retreat of Antarctic outlet glaciers[42–44] has been observed where warm waters from the depths of the Southern Ocean can upwell and be channelized towards the base of ice shelves[26,39,41-45]. Similarly, warm ocean waters have been linked with the retreat of marine-terminating glaciers and ice shelves in the western Antarctic Peninsula since at least the 1990s[46]. The role of subglacial water discharge in ice-shelf basal melting remains poorly constrained, with some research suggesting it can increase basal melting near the grounding zone[47,48].

Both the GrIS and AIS exhibit interannual- to decadal-scale variability in response to oceanic forcing potentially related to internal climate variability[37,49]. A sustained anomaly in oceanic forcing, as simulated for the Amundsen Sea over the 20th century[50], can ultimately perturb an ice sheet until its equilibrium state cannot be recovered under evolving climate conditions. However, a historical dearth of oceanographic measurements precludes a detailed assessment of the precise mechanisms controlling these long-term styles of behaviour.

Effect of sea ice on ice-sheet change

Natural variability in sea-ice cover can also drive changes in ice-sheet mass budget. During the satellite era, ice-shelf advance has been observed when highly pressurised sea ice is connected to the shelf front or tidewater glaciers, which prevents calving through enhanced buttressing and reduced gravitational flow[51,52]. Sea ice cover also limits how much and how far atmospheric moisture reaches inland in the form of snowfall, with important implications for accumulation[53,54]. Prior to the satellite era, records of such processes and their importance for longer-term ice-sheet mass balance can be reconstructed from ice-core proxies[55,56] and marine sediment cores[57] that are used to infer past sea-ice cover and its relationship with changing oceanic and atmospheric frontal systems. For relatively small and thin ice shelves (including the Antarctic Peninsula's Larsen A and B ice shelves prior to their collapse), short-lived, high-energy ocean waves during times of regional, storm-driven sea-ice loss, can also occasionally trigger calving events[51,58].

Ice-sheet hydrology

Surface melt is widespread and complex in both Greenland and on Antarctica's low-lying ice shelves[59,60] (Figure 2). Surface melt has the potential to affect surface mass balance, ice dynamics and ice-shelf collapse. The GrIS experiences considerable mass loss through runoff; models show that on average 50% of ice loss between 1992-2018 occurred via this mechanism[39,61]. There, surface melt can also influence ice dynamics through connections to the subglacial hydrological system[62]. At the ice-bed interface, AIS subglacial hydrology is poorly characterised but has the potential to drive ice-sheet melt and flow, as suggested for the Antarctic Peninsula[63,64]. Akin to the processes driving seasonal GrIS flow, these accelerations have in-part been linked to prolific surface meltwater drainage to the bed[63,64].

In Antarctica, surface melting is widespread only on and immediately adjacent to the continent's ice shelves[28,59], where much of the melt refreezes in-situ so is not lost through runoff[39]. Meltwater can, however, influence ice-shelf stability though the formation of surface meltwater lakes, leading to surface meltwater-driven ice-shelf flexure and/or through-ice fracture ("hydrofracture")[65]. Some Antarctic Peninsula ice shelves have been noted to be particularly vulnerable to hydrofracture, and their future vulnerability will be partly determined by the production and destination of surface melt[66] as well as snowfall rate, which replenishes pore space[67,68]. Ultimately, hydrofracture-driven ice-shelf disintegration events can lead to accelerated ice loss via the de-buttressing of upstream glacier ice[69].

Sudden ice-shelf collapse can be influenced by weather events. For example, the 2002 collapse of Larsen B Ice Shelf was preceded by three months of exceptional surface melting[70]. However, the ice shelf had already been partly primed for collapse by melt ponding[71] and ice-shelf thinning due to basal melting in prior decades[72], suggesting that climatic influences can also provide the foundation for collapse events. Firn aquifers (subsurface meltwater reservoirs) form in both the GrIS[73] and AIS[74]. Like melt ponds, they are sensitive to both climatological accumulation and melt rate[75,76]. In this regard, changes in their extent and volume might also be a useful indicator of ice sheet 'climate'.

In a warming climate, surface melting is likely to become an increasingly important component of ice-sheet mass budget[77,78], partly due to the amplifying melt-albedo feedback[79,80], but this phenomenon might be mitigated on Antarctic grounded ice by snowfall increases[81]. The relationship between climate and the development of surface hydrological systems over multi-annual timescales is still uncertain[82], as is the impact of hydro-dynamic coupling on ice motion for grounded ice[62,83] with large spatial variability expected[84].

Marine Ice Sheet and Ice Cliff Instabilities

In the Amundsen Sea sector of West Antarctica, satellite-derived observations of pervasive grounding-line retreat over the past three decades[23,85,86] have raised concerns of an upcoming onset of a "Marine Ice Sheet Instability" (MISI). MISI is a self-enhancing process that can lead to a rapid and irreversible retreat of grounding lines in regions where the bed topography is below sea level and deepens inland. Several factors can slow down or stop this instability (see Box 1) but it is believed that the current retreat of some glaciers of the Amundsen Sea Sector, such as Thwaites Glacier, may already be undergoing MISI. , MISI would destabilise the marine-based sectors of the AIS in the absence of sufficient ice-shelf buttressing and other pre-conditioning factors[87-90].

In addition to MISI, another potential instability leading to rapid retreat is termed "Marine Ice Cliff Instability" (MICI)[91,92]: a mechanism which could greatly amplify rates of ice-sheet demise via the disintegration of marine terminating glaciers as a function of frontal cliff height. Direct observations of cliff failure are, however, limited, making it difficult to assess whether MICI has ever been at play and how to parameterize the retreat of marine-terminating glaciers in this manner[93]. Box 1 gives some additional details on the mechanisms and importance of MISI and MICI.

Antarctica: 'weather' versus 'climate'

We now provide a wider discussion of short-term fluctuations (sub-daily to decadal) of the AIS, followed by inferred longer-term changes (multi-millennial), projected multi-decadal to multi-centennial changes, and finally the interaction between these short- and long-timescale variations.

Short-term fluctuations

Since the beginning of routine satellite observations in the early 1990s, most of the mass loss of the AIS has occurred in regions exhibiting strong basal melting, retreat, and thinning of ice shelves[23,39–41], implicating oceanic forcing as a key driver (Figure 3b). Interannual to multi-decadal acceleration, thinning and retreat of Antarctic outlet glaciers[42–44,46] has been observed where warm waters from the depths of the Southern Ocean can upwell and be conveyed towards the base of ice shelves[26,39,41-45].

On an hourly to daily basis, tides modulate the amount of oceanic heat that is advected from the open ocean to the AIS' margins[94,95]. Tides can enhance the basal melting of ice shelves[96] causing an additional estimated 4% of ice loss for the entire AIS[97]. Satellite interferometry has revealed that tides also cause short-term fluctuations in grounding line position, resulting in retreats and advances ranging from a few km to more than 15 km[23,85] . Such behaviour is believed to cause oceanic water penetration to and well inland of the grounding zone, increasing oceanic-enabled melting[98,99].

Atmospheric forcing can also have strong short-term variations through, for example, atmospheric rivers, intense accumulation and melt events[100] or other extreme weather events. These extreme events are in turn regionally linked to large-scale modes of atmospheric-ocean circulation variability, especially El Niño tropical Pacific warm episodes and a recently more positive Southern Annular Mode, where teleconnections are in both instances modulated through changes in the Amundsen Sea Low atmospheric pressure system[29]. The direct influence of surface melting on AIS mass loss is negligible at present[39], but is expected to become an increasingly important factor in controlling the overall mass balance of the AIS[59,79]. For example, Larsen B Ice Shelf had been thinning throughout the Holocene[101], to the point that it became vulnerable to the presence of liquid water at its surface. Prior to its 2002 collapse, the ice shelf had two decades of progressive surface lake expansion coinciding with regional climatic warming[72]. The collapse coincided with the drainage of over 2000 surface lakes, which is suggested to have contributed to the break-up event through ice-shelf flexing, weakening and fracturing[71,102,103]. The rapid disintegration of Larsen B instigated prolific inland glacier acceleration due to the loss of buttressing after the collapse of the ice shelf[69,104]. Similar mechanisms, together with enhanced, ocean-driven basal melting, have also been implicated in the break-up of Wilkins Ice Shelf in 2008[105]. Ultimately, the fate of both ice shelves underscores how sustained extreme warm weather events associated with atmospheric river activity, alongside ocean swell-wave induced damage, have the potential to trigger ice-shelf disintegration[10,58,82,106,107].

At interannual timescales, the variability of basal melting of West Antarctic ice shelves over recent decades has been linked to tropical Pacific atmosphere-ocean teleconnections, notably El Niño Southern Oscillation, and to the southward shift and intensification of the westerly winds offshore from Antarctica that regulate the upwelling and advection of Circumpolar Deep Water (CDW) towards the continent[26,108-110]. In other Antarctic sectors over the past decades, interannual variability of basal melt rates has been linked to intrinsic oceanic variability (for example the Totten Glacier in the Indian Ocean sector[111]), and remote connection with the westward shift of the Amundsen Sea Low (for example, the Filchner-Ronne cavity[112]). For an ice sheet in quasi-equilibrium with the climate, these variations in oceanic forcing are not expected to cause significant deviations from the equilibrium state. Indeed, high basal melt rates (>10 m yr^{-1}) do not necessarily imply that the ice shelves and tributary glaciers are out of balance. However, a sustained climate anomaly or long-term trend in oceanic forcing can perturb the system to a new stable state.

Surface melt percolating under grounded ice may also increase ice discharge. For example, rapid intra-annual acceleration of multiple glaciers in the Antarctic Peninsula have been inferred to be controlled by surface meltwater inputs to the subglacial environment[63,64], and there is evidence to suggest that changes in surface climate might directly influence active subglacial hydrological networks in the region[64,113].

Finally, the discharge of icebergs and meltwater in the upper ocean layers has been suggested to temporarily cause an expansion in sea-ice cover[114], which in turn acts to warm subsurface waters through enhanced water mass stratification while lowering near-surface air temperatures around the Antarctic margin[115,116]. This phenomenon also acts to trap warm CDW in intermediate ocean layers, funnelling it towards the undersides of Antarctica's ice shelves where melting is maximised near the grounding line[115-117]. The resulting amplifying feedback on ice loss caused by increased sub-ice shelf melt, and the damping feedback caused by atmospheric cooling, may therefore be important for the AIS's long-term future[91].

Reconstructed longer-term changes

The low-latitude geological record indicates that, during past warm climate time intervals, sea level was higher than at present, implying partial melting of the GIS and AIS. Sea level was more than 7 m higher in the mid-Pliocene Warm Period [3.3 -3 Ma (million years ago)] when atmospheric CO_2 levels peaked above 400 ppm[118,119]. Even during the Early Pleistocene Marine Isotope Stage (MIS) 31 (1.1-1 Ma), the Mid- and Late-Pleistocene MIS 11c (426-396 ka) and MIS 5e (128-116 ka) - when atmospheric CO_2 levels were around or less than 300 ppm and the ocean-continent configuration was similar to today (but the Southern Hemisphere surface temperature exceeded that of today due to astronomical forcing) - sea level was higher than present, implying partial melting of the AIS.

Uncertainties in absolute values of Northern versus Southern ice sheet contribution to past sea-level change obtained from far-field reconstructions can be reduced by direct observations from the Antarctic interior and margins. There, geological archives yield proxies for precipitation, temperature, sea ice, salinity, water depth, and circulation during past interglacials[120]. These data document ice-margin retreat in the Ross Sea and in the Wilkes Subglacial Basin (WSB), East Antarctica, during the warm Pliocene[121,122] and late Pleistocene interglacial intervals[123], when Antarctic air temperatures were at least 2°C higher than pre-industrial levels for ≥2,500 years (Figure 3a). Numerical simulations constrained by ice and sediment cores show that the ice retreated from the WSB around 330,000 and 125,000 ka, coinciding with periods of warmer Southern Ocean conditions and a 4-6-m higher global mean sea level[124] (Figure 3a). If paleo and modern oceanographic data, still lacking in this region, inform about present conditions and confirm these simulations, these findings suggest that even modest (~0.5°C) future warming would be sufficient to cause ice loss from the WSB[125]. Unfortunately, proxy reconstructions can also only be used to approximate a low temporal or spatial resolution climate average state, meaning that while proxies can help to establish ice sheet sensitivity to external climatic forcing, numerical modelling is still relied upon to assess the importance of non-linear variability on AIS processes.

Projected longer-term changes

On decadal to centennial timescales under projected global warming, increasing atmospheric temperatures could result in substantial surface melt over large areas of the GrIS and also AIS, similar to that currently observed in the Canadian Arctic and west Greenland[59,79]. The resulting mass loss is projected to be partly compensated by increases in Antarctic snowfall by 2100, although there remains considerable uncertainty about the magnitude of offset[77,126,127]. Whether or not atmospheric warming could contribute to the disintegration of an entire glacial basin on centennial to millennial timescales remains uncertain[128]. Under future climate warming, models also project increased oceanic heat supply to present-day ice-shelf cavities that are exposed frequently to relatively warm CDW intrusions in the Amundsen Sea[129] and some parts of East Antarctica[130], leading to enhanced basal melt and increased contribution to sea level (Figure 3c). Other, currently cold, ocean cavities (with no or seldom CDW intrusions, for example Filchner-Ronne Ice Shelf's cavity[131-133]) might transition to warm cavities under high greenhouse gas emission scenarios, with potentially important implications for the mass balance of adjoining ice streams and neighbouring ice-sheet drainage areas (Figure 3c).

As alluded to in the previous sections, increases in ocean-driven basal melting, surface ablation or calving rates may lead to widespread ice stream grounding-line retreat[23,92,134–137]. The large Thwaites and Pine Island glaciers in AIS, for example, have seen their grounding lines retreat by more than 1 km yr^{-1} during the satellite era[85,86], and several modelling efforts have suggested that the grounding line of these glaciers could retreat far inland of their present-day position in the future[89,91,138], as they presumably did during the mid-Pliocene Warm Period and/or some of the Pleistocene warm interglacials (Figure 3a). Over longer (multi-centennial) timescales, marine geomorphological evidence has revealed episodes of analogous retreat on the Ross Sea continental shelf, where a 200-km recession of the grounding line from the continental shelf edge occurred over several centuries during the last deglaciation (~11.5 kyr BP[139]). During this time, similar styles of rapid retreat also occurred across the Marguerite Bay region offshore of the Antarctic Peninsula[140]. However, such self-enhancing retreat can be slowed by several local factors[140-142]; for example, otherwise vulnerable grounding lines are known to have re-advanced during the Holocene, once the sea bed rose due to post-glacial isostatic rebound[143].

Notwithstanding local-scale processes, the trigger mechanism for each of the rapid, MISI-like grounding-line migration events detailed above has been ascribed to an array of intermittent, atmosphere-ocean-related forcing events impinging upon the Antarctic coastal margin through time[139,144,145], as well as – in the case of the recent retreat observed in the Amundsen Sector – a likely multi-decadal trend in climatic forcing over at least the past 100 years[146], although internal climate variability is also important[147].

At the continental scale, current ice-sheet models predict a total AIS contribution to sea level rise (relative to the 1995–2014 baseline) of 3-34 cm by 2100 in the case of the high-emission Shared Socioeconomic Pathway (SSP) 5–8.5 (>1000 ppm atmospheric CO_2)[2] (Figure 3c). For a Paris Climate Agreement-like future scenario or better (lower-emission scenarios SSP1–2.6, <450 ppm atmospheric CO2), AIS's contribution is similar to that of SSP5-8.5 by 2100 (sea-level rise = 3–27 cm), but is significantly lower over multi-centennial timescales[2].

As previously discussed, the Marine Ice Cliff Instability (MICI) phenomenon could increase the future mass loss of Antarctica in high-end scenarios. Indeed, explicit parameterization for MICI under SSP5-8.5 is predicted to increase AIS' contribution to sea level rise to 2–56 cm by 2100, but this estimate is uncertain and only based on one model study[91]. Under SSP1–2.6 scenarios, AIS' contributions are again predicted to be similar to that of SSP5-8.5 by 2100[2].

Over much longer (multi-centennial) timescales, the difference between projected sea-level rise for both SSP scenarios clearly emerges. Under SSP1-2.6, the AIS' contribution is up to 78 cm and could reach 135 cm sea-level rise by 2300 if parameterising for MICI[2]. Under SSP5-8.5 scenarios, the projected AIS contribution reaches 3.13 m and up to more than 13 m if MICI is accounted for in the projections[2]. Although the uncertainties related to the knowledge gaps about MISI, MICI and ice-ocean interactions preclude more accurate projections of the AIS's future contribution to sea level, estimates of multi-metre sea-level rise fall within the range of that inferred from geological records for key warm paleo periods[118,119] (Figure 3).

Interaction of short- and long-term changes

Most short-term atmospheric and oceanic fluctuations around Antarctica, causing episodic calving or anomalous snowfall or melt events, are part of the internal variability of the climate system. Since the AIS is not currently in steady state, these short-term variations in atmospheric or oceanic conditions can trigger self-reinforcing (amplifying) feedbacks that ultimately increase the AIS's sensitivity to longer-term climatic forcing. For example, observations of ice flow in the Amundsen Sea Embayment or the collapse of Larsen B ice shelf illustrate that variability in ocean- and atmosphere-induced melting has the potential to trigger ice thinning, retreat or collapse of ice shelves, grounding-line retreat and ice-flow acceleration.

Over much shorter timescales, the marine geomorphological record[148-150] has further revealed that pulses of extremely rapid grounding-line retreat (10s to 100s m per day) can occur in the absence of steeply retrograde bed topography conducive to MISI, and across a period of only days to months (i.e., behaviour potentially reflective of ice-sheet perturbation(s) in response to 'weather'-type forcing). Most notably, this includes an inferred grounding-line retreat rate of up to 50 m per day (equivalent to ≥10 km yr^{-1}) in the Antarctic Peninsula during regional deglaciation of the continental shelf (approximately 10,700 yr BP[148]), which constitutes the highest known rate of retreat in Antarctica. Grounding-line retreat rates nearing this magnitude have, however, now been detected in West Antarctica (~30 m per day over the course of 3.6 months in 2017 at Pope Glacier[135]), offering important corroboration of these inferred magnitudes of retreat.

These marine geomorphological observations ultimately reveal how nonlinear ice-sheet retreat can be, with substantial 'pulses' of grounding-line retreat occurring over short timescales followed by longer periods of relative stability. They also highlight the important role ice sheet bed geometry plays in modulating rates of retreat, with suggestions that flat-bedded parts of ice sheets may be particularly vulnerable to pulses of rapid ungrounding[150]. In the context of Antarctica, the longer-term ice-dynamical response of the ice sheet to such rapid recession remains unknown. Nonetheless, the prolific rates of retreat inferred from these records imply that, even in the absence of MISI/MICI, the future pace of short-term AIS retreat over such vulnerable regions may be significantly greater than most satellite- and model-derived insights suggest.

Greenland 'weather' versus 'climate'

Here we discuss short-term fluctuations (sub-daily to interannual) of the Greenland Ice Sheet, followed by observed longer-term changes (decadal to geological), then projected decadal to centennial changes, and finally the interaction between short- and long- timescale changes.

Short-term fluctuations

Short-term fluctuations in the GrIS mass balance mainly arise from surface melting. Extreme examples linked to climate warming are the record seasonal melt events of summers 2012 and 2019[151], when over a few days to a few weeks ~60-90% of the surface temporarily melted (which had not been seen since at least 1979, the start of the satellite record), and unprecedentedly late seasonal melt in September 2022 that involved 36% of the ice-sheet surface including the Summit station at 3250 m elevation[152]. The 2019 melt event resulted in a record 444 Gt yr^{-1} mass loss, approximately double the average mass loss for the 2010s[153] (Figure 1). Extreme melting is commonly driven by atmospheric blocking, and is also associated with atmospheric river delivery of extreme heat and moisture[154]. The frequency of moisture-laden air masses has increased[155]. As part of an atmospheric river episode, rainfall occurred in mid-August 2021 at Summit, apparently for the first time in modern history, prolonging melt conditions through the ensuing melt-albedo feedback[156]. With Greenland climate warming[157], the melt threshold in the lower atmosphere is more frequently crossed, producing an increasing rainfall fraction of total precipitation[158] (see Figure 4).

Surface meltwater can infiltrate to the bed and increase ice flow. The ice dynamical response to surface melting can occur on diurnal to weekly timescales[159–161], depending on the amount of melt and the seasonally evolving subglacial drainage efficiency, with peak summer speeds often exceeding the annual mean by 25-100% in the fast flowing areas 40 km inland from the GrIS margin[159,162–164].

Tidewater glacier calving allows large-scale mass loss over short timescales. Calving-induced changes in near-terminus stresses can disrupt upstream ice flow on timescales of minutes[165] to days[166,167]. Changes in the frontal position of tidewater glaciers (driven by variation in submarine melting and/or calving) rates) can trigger increases in dynamic mass loss that last several years and have a marked impact on regional mass balance (e.g. ref. 168). Calving is fundamentally controlled by the stress state at the glacier terminus, which can be modified by bed topography[169,170], tidal variation[171,172], submarine melt[173,174], surface meltwater ejection from the grounding line into fjord waters which enhances underwater heat exchange and melting[175], and at the ocean surface the stabilising effect of sea ice and mélange[176,177]. Observations and modelling evidence suggests that short-term surface meltwater variability affects the calving dynamics of Greenland tidewater glaciers[34,175,178] but the net effect is complicated by the listed factors.

Observed longer-term changes

Over 2002-2020, the average mass change of the GrIS was -235±21 Gt yr^{-1} [153]. During 2007-2017, the overall mass loss was estimated to comprise a 64% contribution from surface mass balance and 36% from ice dynamical losses, with the largest rates of GrIS surface elevation change occurring at fast-flowing marine outlets[61]. Reference 179 contends that surface ablation through meltwater runoff is the primary control on the trend and interannual variability of the GrIS mass budget.

A slight increase in surface elevation observed by satellite altimetry in the interior GrIS above 2000 m elevation between 2007 and 2017 suggests that snow accumulation increased during this period of increasing temperatures[61], but surface mass balance models generally underestimate snow accumulation in the interior GrIS[180] and cannot explain the observed interior thickening[61]. Greenland atmospheric warming[157] has been accompanied by melt, runoff and rainfall increases[158,181] that have outpaced the 7% snowfall accumulation increase per degree Celsius warming during 1840 to 1999[182]. In the snow accumulation area, the effect of increased refreezing in the firn has led to an expansion of partly impermeable ice slabs, limiting firn meltwater storage and enhancing lateral runoff through firn[183,184]. This deterioration of the firn layer includes an expansion of the bare ice area across the northern and western GrIS[17,185,186]. Firn deterioration is further augmented by melt and rainwater storage in perennial firn aquifers, and in the south-east of the GrIS, aquifer area has increased[187].

Ice-core paleoclimatic reconstructions of GrIS during the previous interglacial, the Eemian (130-115 kyr before present), suggest the ice sheet is more resilient to increased melting than derived from regional climate model (RCM) projections, with temperatures at 8±4 °C above the mean of the past millennium[188] producing a relatively modest ~2 m sea-level increase. Through the last 11.7 kyrs of the current interglacial, ice-core reconstructions indicate an initial thinning of several hundred m in the northwest and southeast of GrIS over the first few thousand years after the glacial-interglacial transition, while the interior areas have remained stable within a few hundred m through the Holocene[189].

Projected longer-term changes

The current generation of physically-based GrIS sea-level projections is built on a chain of modelling efforts from general circulation model output to regional climate models, ice-sheet models and statistical emulation[2], where uncertainties in all elements are propagated to the final result.

For the SSP5-8.5 high emission scenario, AR6 GrIS model projections[2,77,126] yield a 13.0 cm (with a likely range of 9 to 18 cm) contribution to sea level rise by year 2100. Under a Paris Climate Agreement-like future scenario (SSP2-4.5), the sea-level rise contribution is 8 cm (likely range 4 to 14 cm), 62% of the high emission amount. The two scenarios begin to increasingly diverge after mid-century, with summer air temperature over Greenland differing 0.6°C by 2050 and 2.4°C by 2100 (Figure 4).

The two decades (2002-2022) of observed GrIS mass change[190] (updated data – our Figure 1) indicate an average sea-level rise contribution of 0.70±0.05 mm per year, while another recent study[191] gives 0.61±0.25 mm per year over the same period. These 20-year rates are not reached by the AR6 projections median estimate in the SSP2-4.5 scenario until, respectively, years 2029 to 2049[190] (2022 to 2042[191]) or, in the case of ref. 191, by 2021 to 2041 under SSP5-8.5[2]. This difference of timing between the observed and modelled average rate of change, although within the AR6 error envelope (Figure 4), probably arises from the limitations of the Global Climate Model (GCM) and RCM forcing, the range of Ice Sheet Model

Intercomparison Project 6 (ISMIP6) model results[77], and observed processes not fully incorporated by ice-sheet model projections.

Currently, about half of the surface meltwater on the GrIS is refrozen and retained in the firn in model estimates[192]. Under future warming scenarios, the ability of the firn to retain meltwater could decrease and eventually be lost, and centuries of cold climate would be required for it to be regained. Climate projections show that the refreezing capability could start to permanently decline by year 2100 under the high emission scenario SSP5-8.5[193].

Although RCMs show increasing precipitation over Greenland in a warming climate, it is not certain by how much snow accumulation will increase and projected surface mass balance suggests that surface melt and runoff will far outweigh any increase in accumulation[194–196]. Climate warming has contributed to elevated GrIS snow-line altitude and a mass-budget deficit. Keeping the average deficit realised over the past two decades constant would lead to a sea-level contribution of at least 27±7 cm[179]. While the approach does not provide a timescale for the response, modelling suggests that the GrIS adjusts to surface mass balance perturbations across annual to multi-millennial timescales[197–199].

Interaction of short- and long-term changes

Extreme atmospheric blocking episodes have led to near-record surface meltwater runoff in 2012 and 2019[151]. However, these record atmospheric events were either followed (2013) or preceded (2018) by greatly contrasting melt anomalies, highlighting the role of increased interannual variability on extreme glaciological events and ice-sheet evolution.

The response of tidewater glaciers to atmospheric and oceanic forcing remains a key uncertainty in determining the future mass loss from the GrIS[2]. Over several years, atmospheric circulation anomalies were found to drive a warm ocean current which destabilised the largest west GrIS tidewater glacier[200]. Further connection comes through increasing meltwater runoff driving underwater melting[201]. Seasonal ice-velocity fluctuations are observed at tidewater glaciers, influenced by surface melt and runoff, subglacial hydrology, and ice-ocean interactions at the ice front[164]. While seasonal ice flow variability is a complex response to surface meltwater, basal drainage, calving events and break-up of mélange at the tidewater terminus[162,202], interannual flow variability can be a response to both contemporary terminus retreat or a lagged response to inland changes in snowfall and ice flux[203–205].

Englacial and subglacial water, its transit, heat transfer to ice, lubricating effects on glacier flow, and subglacial storage have received much attention. As infiltration of surface meltwater increases, the extent to which lubricating effects are self-regulating remains a key topic. Global Navigation Satellite System (GNSS) and surface climate measurements in western Greenland[159] confirm an annual cycle in ice flow coupled to surface meltwater production and transport into the subglacial drainage system[206]. The observed ice acceleration decreases as the melt season progresses, indicating the development of an efficient, lower pressure subglacial drainage network[207]. While this self-regulation has now been firmly documented[208,209], it has not been observed more than 40 km inland from the GrIS margin. The efficiency of meltwater routing and subglacial drainage is likely to increase with climate warming and limit the impact of runoff fluctuations on annual ice flow velocities or multiannual acceleration[163,202,210,211] in contrast to their much clearer effect on diurnal to seasonal-scale flow[162–164].

Inland and up to 140 km from the ice margin, where thicker ice and lower surface melt rates occur, persistent ice-flow acceleration has been observed in winter and summer at and above the equilibrium line altitude[212]. The underlying cause appears to be upstream migration of a distributed subglacial drainage along with the potential viscous warming and decoupling of a previously frozen bed. The area over which such meltwater penetration occurs is projected to increase under future climate scenarios[213]. Late melt season rainfall is also implicated in land-terminating glacier acceleration[214]. However, the relatively modest values of ice acceleration involved (~1 m yr^{-1} over 3 years[212]) means this is unlikely to significantly influence mass loss relative to either changes in surface mass balance or the major dynamic changes documented at tidewater glaciers[215].

The many scales of iceberg calving, from the day-to-day crumbling of small bergs to the detachment of large tabular bergs at intervals of years to decades[216], are a continuum connecting the short- and long-term dynamics of marine outlet glaciers. Sustained retreats of calving termini often co-occur with dynamic drawdown of ice from tens of km upstream[217,218]. Numerical models suggest that perturbations of calving termini can initiate long-term, large-scale dynamic changes far into the ice-sheet interior[219]. Glacier outlet geometry, including the ice thickness and the presence or absence of steep "knickpoints" in the bed topography, controls how fast and how far a wave of thinning initiated at the terminus can propagate inland[220]. High-melt years, or consecutive years with high melt and loss of mélange can destabilise the terminus and trigger a rapid dynamical retreat[221]. Such a threshold is where glacier sensitivity to terminus position could depend on tides[171] and near-terminus bed topography, so that normal calving when the terminus is around a susceptible point in the bed could initiate multi-annual retreat[166,222]. Model results further show that failing to account for seasonal- to decadal-scale climate variability can bias the projected multi-decadal mass loss[223,224].

Summary and future perspectives

With both ice sheets having entered a new regime of negative mass balance (Figure 1), and highly uncertain projections for their sea-level contribution(Antarctica especially), it is of utmost importance to continue monitoring the behaviour of both ice sheets using in-situ and spaceborne methods. While we have learned much about the causes, nature and implications of 'weather' vs. 'climate' forcing for ice sheet mass balance from such methods, continued and enhanced monitoring and modelling efforts are required to fully partition their relative importance in driving future ice-sheet demise. Such knowledge, including higher-resolution mass changes, high-elevation, tidewater glacier and ice-shelf hydrology and dynamics, calving, ocean heat flux and grounding zone bed geometry, will be critical for accurately predicting both Greenland and Antarctica's future evolution and contribution to sea level. Below, we discuss further these key unknowns and data requirements in the context of satellite monitoring, in-situ measurements and modelling, and suggest a series of specific, actionable recommendations on how to address them.

Satellite monitoring

Forthcoming spaceborne observing systems will further extend our understanding of short-term change across the polar regions, and include the launch of NISAR (a NASA-Indian Space Research Organization SAR mission; https://nisar.jpl.nasa.gov/) in 2024 and the ESA Harmony mission (https://www.eoportal.org/satellite-missions/harmony) in 2029. Both missions have vastly expanded capabilities to sample the deformation, flow dynamics and grounding line changes of the ice sheets at weekly resolution and with unprecedented precision. It will be essential for the community to use these data for interpretation and to constrain models, provide feedback to the missions, and help design the next generation of satellite sensors.

The NASA/DLR (German Aerospace Center) Gravity Recovery and Climate Experiment mission (GRACE) and its successor GRACE-Follow-On (GRACE-FO) have provided the most accurate, spatially comprehensive and continuous assessment of mass change across the ice sheets since 2002[225] (Figure 1), which are critical for constraining models and projections of sea-level rise. A joint GRACE-FO successor mission between Deutsches GeoForschungsZentrum/Deutsches Zentrum für Luft-und Raumfahrt (GFZ/DLR) and NASA/JPL is scheduled for launch in 2027. This mission will fly an upgraded laser-ranging interferometer, which will improve intra-satellite distance measurements by two orders of magnitude[226], with corresponding enhancements in the spatial and temporal resolution of future mass change observations[226,227]. In parallel, the ESA Ministerial Council has started to engage in the launch of an additional GRACE-FO-type satellite pair in 2031. The framework of both GFZ/DLR-NASA/JPL and ESA satellite pairs flown in a hybrid Bender orbit configuration, termed the Mass change And Geosciences International Constellation (MAGIC)[228], will globally reduce and homogenise uncertainties of sea-level change estimates. Beyond these missions, continued international investment into initiatives such as the EU Copernicus programme and the long-running NASA/USGS Landsat programme will be key towards ensuring long-term continuity in our ability to routinely monitor the ice sheets from space.

Aside from the (multi-)national, space-agency managed Earth Observation programmes mentioned above, an increasing number of commercial companies have recently launched dedicated, ultra-high resolution imaging satellites capable of providing daily to sub-daily visible and radar microwave observations of ice-sheet and ice-shelf rifting, fracturing and iceberg calving at better than 1-m spatial resolution. Such data offer substantial insights not necessarily possible from conventional imaging afforded by, for example, the more moderate resolution Landsat and EU Copernicus/ESA Sentinel constellation of satellites. Despite these opportunities, most commercial satellite imagery presently comes with substantial cost, usage restrictions and/or other access barriers at the ice-sheet scale. We therefore advocate the need for increased dialogue with these companies for the purposes of dedicated and routine commercial satellite image acquisition over the polar regions and open-access use by the international scientific community. Upcoming initiatives such as the International Polar Year 2032/33 can and should act as important catalysts for the commencement of such dialogue and, ultimately, the facilitation of scientific progress.

In-situ observations

To improve our understanding of ocean conditions offshore of Greenland and Antarctica and of sub ice-shelf conditions, autonomous “Argo” floaters (https://argo.ucsd.edu/) are now ready for ice environments and should be urgently deployed to provide a comprehensive observational network across the polar oceans. Argo-derived observations should be complemented by conductivity, temperature and depth (CTD) probes deployed on sea mammals (https://www.meop.net/) and observations of the ice-sheet proximal environment collected using robotic devices[229,230] and other in-situ techniques[231]. Such a network would enable models to constrain ocean state and ice-melt rates at the ice-sheet margins with minimised uncertainty. In Antarctica, the observation network should ideally also extend to the grounding zone, as this is the region most crucial to ice-sheet evolution, most difficult to access, and also the least well observed at present. In Greenland, there is not a single direct measurement of submarine melt rate at a tidewater glacier , and very few indirect measurements, which severely limits our understanding of the importance of submarine melting in these regions. Dedicated field campaigns (e.g. ref. 232) and new technologies/methodologies are needed to address this deficiency.

Knowledge gaps about the Antarctic subglacial topography, especially around grounding zones[233] and on the continental shelf[234] (Figure 3a) under areas of present-day ice-shelf cover, currently preclude understanding of ice-sheet dynamics in response to atmospheric and oceanic forcing in sectors potentially vulnerable to rapid retreat. It is therefore urgent that we improve understanding of the precise geometry and geological composition of the AIS grounding zone at the continental scale, via dedicated in-situ geophysical campaigns such as that proposed by the Scientific Committee on Antarctic Research (SCAR)-funded ‘RINGS’ Action Group (https://www.scar.org/science/rings/about/). Seaward of the present-day grounding zone, we further expect that the collection of systematic bathymetric and subsea-floor information over deglaciated margins will yield important new insights into the configuration and behaviour of ice-sheets past and present[148,150], with additional importance for model boundary setting, validation and uncertainty reduction purposes.

Improving model- and satellite-based estimates of, for example, AIS surface melt and firn hydrology will require a similar (and substantially increased) network of surface-based 'energy balance-enabled' weather stations, operating radiation sensors. A similar effort on the GrIS under the guidance of the Geological Survey of Denmark and Greenland has led to excellent ice-sheet wide coverage from around 2010, enabling the calibration of satellite-based surface melt rate estimates using machine learning techniques[235]. And finally, improving model representations of ice-shelf flexure and hydrofracture in response to surface meltwater ponding and drainage, urgently requires additional arrays of in-situ observations. Valuable observations could include water-pressure measurements to monitor lake depths, arrays of GNSS stations to quantify ice-shelf flexure (e.g. ref. 236), and seismic data to give insights into fracturing and rifting.

Ice-sheet modelling

A major challenge for the modelling community lies in capturing the long-term essence of ice-sheet dynamics occurring at continental to global scale and short-term response occurring at local to regional scales within the same simulation. More sophisticated ice-sheet models – constrained directly using knowledge gleaned from both the satellite and marine geomorphological records as well as in-situ field observations – are needed to better predict future trends of rapid ice-sheet evolution. Observationally constrained, regional-scale process models[160,236] have yet to be upscaled to the ice-sheet scale, underscoring the requirement for comprehensive in-situ-based observations to help improve model-based predictions of the rate at which the ice sheets will respond to 'weather' versus 'climate' forcing.

The processes that models do not currently explicitly simulate include decreased permeability of firn layers[183], amplified melt due to biological snow and ice darkening[237], tidewater glacier acceleration and destabilisation by submarine melting[37,238,239], loss of the buttressing effect from ice shelves[240], accelerating interior motion from increased melt and rainfall[214], enhanced basal thawing due to hydraulically-released latent heat and viscous warming[241], and ice-shelf flexure, (hydro)fracture and collapse in response to surface meltwater ponding and drainage[72,103,236]. The aforementioned spectrum of processes not currently included in the modelling chain leads to deep uncertainty, and could give rise to additional sea-level contributions, represented by the high-end storyline in AR6[2] or high-end mass loss estimates in ref. 242.

GCM and Earth System Model projections typically under-represent changes in atmospheric circulation and wind that are associated with increased Greenland atmospheric blocking[243,244] (Figure 5), which means that projected surface melt increase of the GrIS could be misrepresented if such summer circulation changes that have been observed since the 1990s persist in the next decades[245].

Accurately simulating calving and damage processes using physics-based treatments is one of the greatest current challenges in ice-sheet modelling. The lack of a unified, physics-based treatment of calving processes in models continues to contribute to the deep uncertainty surrounding sea-level projections for both ice sheets, especially the AIS[2,246]. In particular, the highest sea-level projections currently included in AR6 are produced by numerical simulations that contain a representation of MICI which results in sea-level rise estimates that are an order of magnitude higher than simulations without MICI[1]. However, these projections are based on a simplified, untested and unverified implementation of MICI in a single ice-sheet model[128], requiring two separate calving mechanisms: ice-shelf collapse caused by hydrofracturing, followed by potential cliff failure[92,93]. At present there is no scientific consensus about the physical basis and exact formulation of these mechanisms in simulations of large-scale ice sheet dynamics. Attempts have been made to implement calving laws and damage mechanisms in ice-sheet models[93,247,248]. However, in the ISMIP6 sea-level projections, AIS calving and damage are not considered in any ice-sheet model[138]., although ISMIP6 GrIS simulations did include a heavily parameterised representation of retreat due to calving and submarine melting[77]. Therefore, there is an urgent need to improve the physical representation of ice-sheet and ice-shelf fracture, validate calving laws and implement robust damage mechanics algorithms in numerical ice-sheet models, although such improvement will need to overcome the mismatch between the scales of fracture and calving processes and the resolution of ice-sheet scale models. Alongside investment in model development, the remotely sensed and in-situ data sources outlined above offer an important opportunity for model validation for this purpose.

Model representation of sub-shelf melting is another key challenge. Despite the development of sophisticated coupled ice-ocean models[133,249], which have greatly improved the ability to represent melt rates for complex time-evolving geometries and ocean properties, a number of challenges remain. To increase confidence in the representation of melt rates near the grounding line, where ice dynamics are particularly sensitive to basal melt, high-resolution numerical simulations constrained by satellite- and in-situ-based observations of past and present basal melt and seafloor bathymetry are required. Secondly, the two-way interaction between changes in ice-shelf geometry (thinning, thickening and calving) and basal melt rates are key to simulating future mass loss from the AIS[137,250], yet these feedbacks remain poorly understood. For the GrIS, it is not yet possible to meaningfully couple ice sheet and ocean models across the ~200 complex fjord systems, which fall below the resolution of regional ocean models, with a need for alternative methods to bridge this gap. Improved observations of melt rates for changing cavity shapes and ocean conditions at annual to centennial timescales are thus a fundamental research priority.

Due to the high computational cost of coupled ice-ocean simulations, most sea-level projections are currently based on stand-alone ice-sheet model simulations that use a range of simplified melt parameterisations. Not only do spatial melt patterns vary greatly between these parameterisations, but recent AIS projections[126,138,251] have also revealed that their sensitivity to changes in ocean temperature constitutes a major source of uncertainty. This limitation needs to be addressed by developing new calibration approaches based on transient ocean model simulations[252,253].

Co-ordinated ice-sheet modelling exercises such as ISMIP6/7 are largely unfunded, community-driven efforts: therefore, given the above-mentioned limitations with models, we strongly advocate funding this kind of co-ordinated modelling exercise. Finally, another recent advance that is becoming increasingly important in ice-sheet modelling is the development and implementation of coupled ice sheet-Earth system models, such as UKESM and CESM2/3[127,254,255], where ice sheets are able to dynamically interact with the climate and wider Earth system. Ice sheet and coupled models can complement each other to fully realise and shed light upon ‘weather’ vs. ‘climate’ in a truly interconnected, global sense.

References

1. Hanna, E. *et al.* Mass balance of the ice sheets and glaciers – Progress since AR5 and challenges. *Earth-Science Reviews* vol. 201 102976 Preprint at https://doi.org/10.1016/j.earscirev.2019.102976 (2020).
2. Fox-Kemper, B., Hewitt, H. T. & Xiao, C. Ocean, Cryosphere and Sea Level Change. in *IPCC: Climate Change 2021: The Physical Science Basis. Contribution of Working Group I to the Sixth Assessment Report of the Intergovernmental Panel on Climate Change* (eds. Masson-Delmotte, V. et al.) 1211–1361 (Cambridge University Press, 2021).
3. Elvidge, A. D. *et al.* Foehn jets over the Larsen C Ice Shelf, Antarctica. *Quarterly Journal of the Royal Meteorological Society* vol. 141 698–713 Preprint at https://doi.org/10.1002/qj.2382 (2015).
4. Ekaykin, A. A., Kozachek, A. V., Ya. Lipenkov, V. & Shibaev, Y. A. Multiple climate shifts in the Southern Hemisphere over the past three centuries based on central Antarctic snow pits and core studies. *Ann. Glaciol.* **55**, 259–266 (2014).
5. Ekaykin, A. A. *et al.* The changes in isotope composition and accumulation of snow at Vostok station, East Antarctica, over the past 200 years. *Ann. Glaciol.* **39**, 569–575 (2004).
6. Richter, A. *et al.* Surface Mass Balance Models Vs. Stake Observations: A Comparison in the Lake Vostok Region, Central East Antarctica. *Front Earth Sci. Chin.* **9**, (2021).
7. Box, J. E. *et al.* Greenland Ice Sheet Rainfall, Heat and Albedo Feedback Impacts From the Mid-August 2021 Atmospheric River. *Geophysical Research Letters* vol. 49 Preprint at https://doi.org/10.1029/2021gl097356 (2022).
8. Lenaerts, J. T. M., Medley, B., van den Broeke, M. R. & Wouters, B. Observing and

Modeling Ice Sheet Surface Mass Balance. *Rev. Geophys.* **57**, 376–420 (2019).

9. Maclennan, M. L., Lenaerts, J. T. M., Shields, C. & Wille, J. D. Contribution of Atmospheric Rivers to Antarctic Precipitation. *Geophys. Res. Lett.* **49**, e2022GL100585 (2022).

10. Wille, J. D. *et al.* Antarctic Atmospheric River Climatology and Precipitation Impacts. *Journal of Geophysical Research: Atmospheres* vol. 126 Preprint at https://doi.org/10.1029/2020jd033788 (2021).

11. Mattingly, K. S., Mote, T. L. & Fettweis, X. Atmospheric River Impacts on Greenland Ice Sheet Surface Mass Balance. *Journal of Geophysical Research: Atmospheres* vol. 123 8538–8560 Preprint at https://doi.org/10.1029/2018jd028714 (2018).

12. Grazioli, J. *et al.* Katabatic winds diminish precipitation contribution to the Antarctic ice mass balance. *Proceedings of the National Academy of Sciences* vol. 114 10858–10863 Preprint at https://doi.org/10.1073/pnas.1707633114 (2017).

13. Das, I. *et al.* Influence of persistent wind scour on the surface mass balance of Antarctica. *Nature Geoscience* vol. 6 367–371 Preprint at https://doi.org/10.1038/ngeo1766 (2013).

14. Medley, B., Lenaerts, J. T. M., Dattler, M., Keenan, E. & Wever, N. Predicting Antarctic Net Snow Accumulation at the Kilometer Scale and Its Impact on Observed Height Changes. *Geophys. Res. Lett.* **49**, e2022GL099330 (2022).

15. Hanna, E., Cropper, T. E., Hall, R. J., Cornes, R. C. & Barriendos, M. Extended North Atlantic Oscillation and Greenland Blocking indices 1800–2020 from new meteorological reanalysis. *Atmosphere* **13**, 436 (2022).

16. Hofer, S., Tedstone, A. J., Fettweis, X. & Bamber, J. L. Decreasing cloud cover drives the recent mass loss on the Greenland Ice Sheet. *Sci Adv* **3**, e1700584 (2017).

17. Noël, B., van de Berg, W. J., Lhermitte, S. & van den Broeke, M. R. Rapid ablation zone expansion amplifies north Greenland mass loss. *Science Advances* vol. 5 Preprint at https://doi.org/10.1126/sciadv.aaw0123 (2019).
18. Hermann, M., Papritz, L. & Wernli, H. Lagrangian Analysis of the Dynamical and Thermodynamic Drivers of Greenland Melt Events during 1979-2017. Preprint at https://doi.org/10.5194/egusphere-egu2020-13492.
19. Ding, Q. *et al.* Tropical forcing of the recent rapid Arctic warming in northeastern Canada and Greenland. *Nature* **509**, 209–212 (2014).
20. Shahi, S., Abermann, J., Heinrich, G., Prinz, R. & Schöner, W. Regional Variability and Trends of Temperature Inversions in Greenland. *J. Clim.* **33**, 9391–9407 (2020).
21. Tedesco, M. *et al.* The darkening of the Greenland ice sheet: trends, drivers, and projections (1981–2100). *Cryosphere* **10**, 477–496 (2016).
22. Van Tricht, K. *et al.* Clouds enhance Greenland ice sheet meltwater runoff. *Nat. Commun.* **7**, 10266 (2016).
23. Rignot, E. *et al.* Four decades of Antarctic Ice Sheet mass balance from 1979–2017. *Proceedings of the National Academy of Sciences* **116**, 1095–1103 (2019).
24. Perren, B. B. *et al.* Southward migration of the Southern Hemisphere westerly winds corresponds with warming climate over centennial timescales. *Commun. Earth Environ.* **1**, (2020).
25. Verfaillie, D. *et al.* The circum-Antarctic ice-shelves respond to a more positive Southern Annular Mode with regionally varied melting. *Commun. Earth Environ.* **3**, (2022).
26. Steig, E. J., Ding, Q., Battisti, D. S. & Jenkins, A. Tropical forcing of Circumpolar Deep Water Inflow and outlet glacier thinning in the Amundsen Sea Embayment, West

Antarctica. *Annals of Glaciology* vol. 53 19–28 Preprint at https://doi.org/10.3189/2012aog60a110 (2012).

27. Medley, B. & Thomas, E. R. Increased snowfall over the Antarctic Ice Sheet mitigated twentieth-century sea-level rise. *Nature Climate Change* vol. 9 34–39 Preprint at https://doi.org/10.1038/s41558-018-0356-x (2019).
28. Banwell, A. F., Wever, N., Dunmire, D. & Picard, G. Quantifying antarctic-wide ice-shelf surface melt volume using microwave and firn model data: 1980 to 2021. *Geophys. Res. Lett.* **50**, (2023).
29. Turner, J. *et al.* The dominant role of extreme precipitation events in antarctic snowfall variability. *Geophys. Res. Lett.* **46**, 3502–3511 (2019).
30. Munneke, P. K. *et al.* Elevation change of the Greenland Ice Sheet due to surface mass balance and firn processes, 1960–2014. *The Cryosphere* vol. 9 2009–2025 Preprint at https://doi.org/10.5194/tc-9-2009-2015 (2015).
31. van den Broeke, M. Depth and Density of the Antarctic Firn Layer. *Arctic, Antarctic, and Alpine Research* vol. 40 432–438 Preprint at https://doi.org/10.1657/1523-0430(07-021)[broeke]2.0.co;2 (2008).
32. Slater, D. A. & Straneo, F. Submarine melting of glaciers in Greenland amplified by atmospheric warming. *Nature Geoscience* vol. 15 794–799 Preprint at https://doi.org/10.1038/s41561-022-01035-9 (2022).
33. Straneo, F. & Heimbach, P. North Atlantic warming and the retreat of Greenland's outlet glaciers. *Nature* vol. 504 36–43 Preprint at https://doi.org/10.1038/nature12854 (2013).
34. Fried, M. J. *et al.* Reconciling Drivers of Seasonal Terminus Advance and Retreat at 13 Central West Greenland Tidewater Glaciers. *J. Geophys. Res.* **123**, 1590–1607 (2018).

35. O'Leary, M. & Christoffersen, P. Calving on tidewater glaciers amplified by submarine frontal melting. *Cryosphere* **7**, 119–128 (2013).

36. Catania, G. A., Stearns, L. A., Moon, T. A., Enderlin, E. M. & Jackson, R. H. Future Evolution of Greenland's Marine-Terminating Outlet Glaciers. *Journal of Geophysical Research: Earth Surface* vol. 125 Preprint at https://doi.org/10.1029/2018jf004873 (2020).

37. Wood, M. *et al.* Ocean forcing drives glacier retreat in Greenland. *Sci Adv* **7**, (2021).

38. Bindschadler, R. *et al.* Getting around Antarctica: new high-resolution mappings of the grounded and freely-floating boundaries of the Antarctic ice sheet created for the International Polar Year. *The Cryosphere* vol. 5 569–588 Preprint at https://doi.org/10.5194/tc-5-569-2011 (2011).

39. Smith, B. *et al.* Pervasive ice sheet mass loss reflects competing ocean and atmosphere processes. *Science* **368**, 1239–1242 (2020).

40. Greene, C. A., Gardner, A. S., Schlegel, N.-J. & Fraser, A. D. Antarctic calving loss rivals ice-shelf thinning. *Nature* vol. 609 948–953 Preprint at https://doi.org/10.1038/s41586-022-05037-w (2022).

41. Pritchard, H. D. *et al.* Antarctic ice-sheet loss driven by basal melting of ice shelves. *Nature* **484**, 502–505 (2012).

42. Miles, B. W. J., Stokes, C. R. & Jamieson, S. S. R. Pan-ice-sheet glacier terminus change in East Antarctica reveals sensitivity of Wilkes Land to sea-ice changes. *Sci Adv* **2**, e1501350 (2016).

43. Greene, C. A., Blankenship, D. D., Gwyther, D. E., Silvano, A. & van Wijk, E. Wind causes Totten Ice Shelf melt and acceleration. *Sci Adv* **3**, e1701681 (2017).

44. Christie, F. D. W., Steig, E. J., Gourmelen, N., Tett, S. F. B. & Bingham, R. G. Inter-

decadal climate variability induces differential ice response along Pacific-facing West Antarctica. *Nat. Commun.* **14**, 93 (2023).

45. Herraiz-Borreguero, L. & Naveira Garabato, A. C. Poleward shift of Circumpolar Deep Water threatens the East Antarctic Ice Sheet. *Nature Climate Change* vol. 12 728–734 Preprint at https://doi.org/10.1038/s41558-022-01424-3 (2022).
46. Cook, A. J. *et al.* Ocean forcing of glacier retreat in the western Antarctic Peninsula. *Science* **353**, 283–286 (2016).
47. Nakayama, Y., Cai, C. & Seroussi, H. Impact of Subglacial Freshwater Discharge on Pine Island Ice Shelf. *Geophysical Research Letters* vol. 48 Preprint at https://doi.org/10.1029/2021gl093923 (2021).
48. Dow, C. F., Ross, N., Jeofry, H., Siu, K. & Siegert, M. J. Antarctic basal environment shaped by high-pressure flow through a subglacial river system. *Nature Geoscience* vol. 15 892–898 Preprint at https://doi.org/10.1038/s41561-022-01059-1 (2022).
49. Jenkins, A. *et al.* West Antarctic Ice Sheet retreat in the Amundsen Sea driven by decadal oceanic variability. *Nature Geoscience* vol. 11 733–738 Preprint at https://doi.org/10.1038/s41561-018-0207-4 (2018).
50. Naughten, K. A. *et al.* Simulated Twentieth-Century Ocean Warming in the Amundsen Sea, West Antarctica. *Geophysical Research Letters* vol. 49 Preprint at https://doi.org/10.1029/2021gl094566 (2022).
51. Christie, F. D. W. *et al.* Antarctic ice-shelf advance driven by anomalous atmospheric and sea-ice circulation. *Nat. Geosci.* **15**, 356–362 (2022).
52. Aoki, S. Breakup of land-fast sea ice in Lützow-Holm Bay, East Antarctica, and its teleconnection to tropical Pacific sea surface temperatures. *Geophysical Research Letters* vol. 44 3219–3227 Preprint at https://doi.org/10.1002/2017gl072835 (2017).

53. Bromwich, D. H., Chen, B. & Hines, K. M. Global atmospheric impacts induced by year-round open water adjacent to Antarctica. *Journal of Geophysical Research: Atmospheres* vol. 103 11173–11189 Preprint at https://doi.org/10.1029/98jd00624 (1998).

54. Wu, X., Budd, W. F., Lytle, V. I. & Massom, R. A. The effect of snow on Antarctic sea ice simulations in a coupled atmosphere-sea ice model. *Climate Dynamics* vol. 15 127–143 Preprint at https://doi.org/10.1007/s003820050272 (1999).

55. Spolaor, A. *et al.* Halogen species record Antarctic sea ice extent over glacial–interglacial periods. *Atmospheric Chemistry and Physics* vol. 13 6623–6635 Preprint at https://doi.org/10.5194/acp-13-6623-2013 (2013).

56. Landais, A. *et al.* Interglacial Antarctic–Southern Ocean climate decoupling due to moisture source area shifts. *Nature Geoscience* vol. 14 918–923 Preprint at https://doi.org/10.1038/s41561-021-00856-4 (2021).

57. Crosta, X. *et al.* Antarctic sea ice over the past 130,000 years, Part 1: A review of what proxy records tell us. Preprint at https://doi.org/10.5194/egusphere-2022-99.

58. Massom, R. A. *et al.* Antarctic ice shelf disintegration triggered by sea ice loss and ocean swell. *Nature* **558**, 383–389 (2018).

59. Bell, R. E., Banwell, A. F., Trusel, L. D. & Kingslake, J. Antarctic surface hydrology and impacts on ice-sheet mass balance. *Nature Climate Change* vol. 8 1044–1052 Preprint at https://doi.org/10.1038/s41558-018-0326-3 (2018).

60. Nienow, P. W., Sole, A. J., Slater, D. A. & Cowton, T. R. Recent Advances in Our Understanding of the Role of Meltwater in the Greenland Ice Sheet System. *Current Climate Change Reports* vol. 3 330–344 Preprint at https://doi.org/10.1007/s40641-017-0083-9 (2017).

61. IMBIE Team. Mass balance of the Greenland Ice Sheet from 1992 to 2018. *Nature* **579**, 233–239 (2020).

62. Williams, J. J., Gourmelen, N. & Nienow, P. Dynamic response of the Greenland ice sheet to recent cooling. *Sci. Rep.* **10**, 1647 (2020).

63. Tuckett, P. A. *et al.* Rapid accelerations of Antarctic Peninsula outlet glaciers driven by surface melt. *Nat. Commun.* **10**, 4311 (2019).

64. Boxall, K., Christie, F. D. W., Willis, I. C., Wuite, J. & Nagler, T. Seasonal land-ice-flow variability in the Antarctic Peninsula. *The Cryosphere* vol. 16 3907–3932 Preprint at https://doi.org/10.5194/tc-16-3907-2022 (2022).

65. Banwell, A. F. & Macayeal, D. R. Ice-shelf fracture due to viscoelastic flexure stress induced by fill/drain cycles of supraglacial lakes. *Antarctic Science* vol. 27 587–597 Preprint at https://doi.org/10.1017/s0954102015000292 (2015).

66. Lai, C.-Y. *et al.* Vulnerability of Antarctica's ice shelves to meltwater-driven fracture. *Nature* **584**, 574–578 (2020).

67. van Wessem, J. M., van den Broeke, M. R., Wouters, B. & Lhermitte, S. Variable temperature thresholds of melt pond formation on Antarctic ice shelves. *Nature Climate Change* vol. 13 161–166 Preprint at https://doi.org/10.1038/s41558-022-01577-1 (2023).

68. Alley, K. E., Scambos, T. A., Miller, J. Z., Long, D. G. & MacFerrin, M. Quantifying vulnerability of Antarctic ice shelves to hydrofracture using microwave scattering properties. *Remote Sensing of Environment* vol. 210 297–306 Preprint at https://doi.org/10.1016/j.rse.2018.03.025 (2018).

69. Scambos, T. A. Glacier acceleration and thinning after ice shelf collapse in the Larsen B embayment, Antarctica. *Geophys. Res. Lett.* **31**, (2004).

70. van den Broeke, M. Strong surface melting preceded collapse of Antarctic Peninsula ice shelf. *Geophysical Research Letters* vol. 32 Preprint at https://doi.org/10.1029/2005gl023247 (2005).

71. Banwell, A. F., MacAyeal, D. R. & Sergienko, O. V. Breakup of the Larsen B Ice Shelf triggered by chain reaction drainage of supraglacial lakes. *Geophys. Res. Lett.* **40**, 5872–5876 (2013).

72. Leeson, A. A., Forster, E., Rice, A., Gourmelen, N. & Wessem, J. M. Evolution of supraglacial lakes on the Larsen B ice shelf in the decades before it collapsed. *Geophys. Res. Lett.* **47**, (2020).

73. Forster, R. R., Box, J. E., Van Den Broeke, M. R. & Miège, C. Extensive liquid meltwater storage in firn within the Greenland ice sheet. *Nature* (2014).

74. Montgomery, L. *et al.* Hydrologic properties of a highly permeable firn aquifer in the Wilkins ice shelf, Antarctica. *Geophys. Res. Lett.* **47**, (2020).

75. Munneke, P. K., M. Ligtenberg, S. R., van den Broeke, M. R., van Angelen, J. H. & Forster, R. R. Explaining the presence of perennial liquid water bodies in the firn of the Greenland Ice Sheet. *Geophys. Res. Lett.* **41**, 476–483 (2014).

76. Harper, J., Humphrey, N., Pfeffer, W. T., Brown, J. & Fettweis, X. Greenland ice-sheet contribution to sea-level rise buffered by meltwater storage in firn. *Nature* **491**, 240–243 (2012).

77. Goelzer, H. *et al.* The future sea-level contribution of the Greenland ice sheet: a multi-model ensemble study of ISMIP6. *Cryosphere* **14**, 3071–3096 (2020).

78. Payne, A. J. *et al.* Future sea level change under coupled model intercomparison project phase 5 and phase 6 scenarios from the Greenland and antarctic ice sheets. *Geophys. Res. Lett.* **48**, (2021).

79. Trusel, L. D. *et al.* Divergent trajectories of Antarctic surface melt under two twenty-first-century climate scenarios. *Nature Geoscience* vol. 8 927–932 Preprint at https://doi.org/10.1038/ngeo2563 (2015).

80. Jakobs, C. L., Reijmer, C. H., van den Broeke, M. R., van de Berg, W. J. & van Wessem, J. M. Spatial Variability of the Snowmelt-Albedo Feedback in Antarctica. *Journal of Geophysical Research: Earth Surface* vol. 126 Preprint at https://doi.org/10.1029/2020jf005696 (2021).

81. Kittel, C. *et al.* Diverging future surface mass balance between the Antarctic ice shelves and grounded ice sheet. *Cryosphere* **15**, 1215–1236 (2021).

82. Arthur, J. F., Stokes, C., Jamieson, S. S. R., Rachel Carr, J. & Leeson, A. A. Recent understanding of Antarctic supraglacial lakes using satellite remote sensing. *Progress in Physical Geography: Earth and Environment* vol. 44 837–869 Preprint at https://doi.org/10.1177/0309133320916114 (2020).

83. Payne, T., Nowicki, S., Goelzer, H. & ISMIP6 team. Contrasting contributions to future sea level under CMIP5 and CMIP6 scenarios from the Greenland and Antarctic ice sheets. Preprint at https://doi.org/10.5194/egusphere-egu2020-11667.

84. Grinsted, A. *et al.* The Transient Sea Level Response to External Forcing in CMIP6 Models. *Earths Future* **10**, e2022EF002696 (2022).

85. Milillo, P. *et al.* Heterogeneous retreat and ice melt of Thwaites Glacier, West Antarctica. *Sci Adv* **5**, eaau3433 (2019).

86. Park, J. W. *et al.* Sustained retreat of the Pine Island Glacier. *Geophysical Research Letters* vol. 40 2137–2142 Preprint at https://doi.org/10.1002/grl.50379 (2013).

87. Rignot, E., Mouginot, J., Morlighem, M., Seroussi, H. & Scheuchl, B. Widespread, rapid grounding line retreat of Pine Island, Thwaites, Smith, and Kohler glaciers, West

Antarctica, from 1992 to 2011. *Geophysical Research Letters* vol. 41 3502–3509 Preprint at https://doi.org/10.1002/2014gl060140 (2014).

88. Feldmann, J. & Levermann, A. Collapse of the West Antarctic Ice Sheet after local destabilization of the Amundsen Basin. *Proc. Natl. Acad. Sci. U. S. A.* **112**, 14191–14196 (2015).

89. Joughin, I., Smith, B. E. & Medley, B. Marine ice sheet collapse potentially under way for the Thwaites Glacier Basin, West Antarctica. *Science* **344**, 735–738 (2014).

90. Schoof, C. Ice sheet grounding line dynamics: Steady states, stability, and hysteresis. *Journal of Geophysical Research: Earth Surface* **112**, (2007).

91. DeConto, R. M. *et al.* The Paris Climate Agreement and future sea-level rise from Antarctica. *Nature* **593**, 83–89 (2021).

92. Pollard, D., DeConto, R. M. & Alley, R. B. Potential Antarctic Ice Sheet retreat driven by hydrofracturing and ice cliff failure. *Earth and Planetary Science Letters* vol. 412 112–121 Preprint at https://doi.org/10.1016/j.epsl.2014.12.035 (2015).

93. Crawford, A. J. *et al.* Marine ice-cliff instability modeling shows mixed-mode ice-cliff failure and yields calving rate parameterization. *Nat. Commun.* **12**, 1–9 (2021).

94. Padman, L., Howard, S. L., Orsi, A. H. & Muench, R. D. Tides of the northwestern Ross Sea and their impact on dense outflows of Antarctic Bottom Water. *Deep Sea Res. Part 2 Top. Stud. Oceanogr.* **56**, 818–834 (2009).

95. Stewart, A. L., Klocker, A. & Menemenlis, D. Circum-antarctic shoreward heat transport derived from an eddy- and tide-resolving simulation. *Geophys. Res. Lett.* **45**, 834–845 (2018).

96. Padman, L., Siegfried, M. R. & Fricker, H. A. Ocean tide influences on the antarctic and Greenland ice sheets. *Rev. Geophys.* **56**, 142–184 (2018).

97. Richter, O., Gwyther, D. E., King, M. A. & Galton-Fenzi, B. K. The impact of tides on Antarctic ice shelf melting. *Cryosphere* **16**, 1409–1429 (2022).

98. Chen, H., Rignot, E., Scheuchl, B. & Ehrenfeucht, S. Grounding zone of Amery ice shelf, Antarctica, from differential synthetic-aperture radar interferometry. *Geophys. Res. Lett.* **50**, (2023).

99. Ciracì, E. *et al.* Melt rates in the kilometer-size grounding zone of Petermann Glacier, Greenland, before and during a retreat. *Proc. Natl. Acad. Sci. U. S. A.* **120**, e2220924120 (2023).

100. Davison, B. J. *et al.* Sea level rise from West Antarctic mass loss significantly modified by large snowfall anomalies. *Nat. Commun.* **14**, 1479 (2023).

101. Domack, E. *et al.* Stability of the Larsen B ice shelf on the Antarctic Peninsula during the Holocene epoch. *Nature* **436**, 681–685 (2005).

102. Scambos, T. A., Hulbe, C., Fahnestock, M. & Bohlander, J. The link between climate warming and break-up of ice shelves in the Antarctic Peninsula. *J. Glaciol.* **46**, 516–530 (2000).

103. Robel, A. A. & Banwell, A. F. A speed limit on ice shelf collapse through hydrofracture. *Geophys. Res. Lett.* **46**, 12092–12100 (2019).

104. Pritchard, H. D. & Vaughan, D. G. Widespread acceleration of tidewater glaciers on the Antarctic Peninsula. *Journal of Geophysical Research* vol. 112 Preprint at https://doi.org/10.1029/2006jf000597 (2007).

105. Scambos, T. *et al.* Ice shelf disintegration by plate bending and hydro-fracture: Satellite observations and model results of the 2008 Wilkins ice shelf break-ups. *Earth and Planetary Science Letters* vol. 280 51–60 Preprint at https://doi.org/10.1016/j.epsl.2008.12.027 (2009).

106. Wille, J. D. *et al.* Intense atmospheric rivers can weaken ice shelf stability at the Antarctic Peninsula. *Commun. Earth Environ.* **3**, (2022).

107. Bozkurt, D., Rondanelli, R., Marín, J. C. & Garreaud, R. Foehn event triggered by an atmospheric river underlies record-setting temperature along continental Antarctica. *J. Geophys. Res.* **123**, 3871–3892 (2018).

108. Adusumilli, S., Fricker, H. A., Medley, B., Padman, L. & Siegfried, M. R. Interannual variations in meltwater input to the Southern Ocean from Antarctic ice shelves. *Nat. Geosci.* **13**, 616–620 (2020).

109. Jenkins, A. *et al.* Decadal Ocean Forcing and Antarctic Ice Sheet Response: Lessons from the Amundsen Sea. *Oceanography* vol. 29 106–117 Preprint at https://doi.org/10.5670/oceanog.2016.103 (2016).

110. Paolo, F. S. *et al.* Response of Pacific-sector Antarctic ice shelves to the El Niño/Southern Oscillation. *Nature Geoscience* vol. 11 121–126 Preprint at https://doi.org/10.1038/s41561-017-0033-0 (2018).

111. Gwyther, D. E., O'Kane, T. J., Galton-Fenzi, B. K., Monselesan, D. P. & Greenbaum, J. S. Intrinsic processes drive variability in basal melting of the Totten Glacier Ice Shelf. *Nat. Commun.* **9**, 3141 (2018).

112. Hattermann, T. *et al.* Observed interannual changes beneath Filchner-Ronne Ice Shelf linked to large-scale atmospheric circulation. *Nat. Commun.* **12**, 2961 (2021).

113. Hodgson, D. A., Jordan, T. A., Ross, N., Riley, T. R. & Fretwell, P. T. Drainage and refill of an Antarctic Peninsula subglacial lake reveal an active subglacial hydrological network. *Cryosphere* **16**, 4797–4809 (2022).

114. Bintanja, R., van de Wal, R. S. W. & Oerlemans, J. Modelled atmospheric temperatures and global sea levels over the past million years. *Nature* **437**, 125–128 (2005).

115. Bronselaer, B. *et al.* Change in future climate due to Antarctic meltwater. *Nature* **564**, 53–58 (2018).

116. Sadai, S., Condron, A., DeConto, R. & Pollard, D. Future climate response to Antarctic Ice Sheet melt caused by anthropogenic warming. *Sci Adv* **6**, (2020).

117. Silvano, A. *et al.* Freshening by glacial meltwater enhances melting of ice shelves and reduces formation of Antarctic Bottom Water. *Sci Adv* **4**, eaap9467 (2018).

118. Dutton, A. *et al.* SEA-LEVEL RISE. Sea-level rise due to polar ice-sheet mass loss during past warm periods. *Science* **349**, aaa4019 (2015).

119. Dumitru, O. A. *et al.* Constraints on global mean sea level during Pliocene warmth. *Nature* **574**, 233–236 (2019).

120. Sangiorgi, F. *et al.* Southern Ocean warming and Wilkes Land ice sheet retreat during the mid-Miocene. *Nat. Commun.* **9**, 317 (2018).

121. Naish, T. *et al.* Obliquity-paced Pliocene West Antarctic ice sheet oscillations. *Nature* **458**, 322–328 (2009).

122. Cook, C. P. *et al.* Dynamic behaviour of the East Antarctic ice sheet during Pliocene warmth. *Nat. Geosci.* **6**, 765–769 (2013).

123. Wilson, D. J. *et al.* Ice loss from the East Antarctic Ice Sheet during late Pleistocene interglacials. *Nature* **561**, 383–386 (2018).

124. Crotti, I. *et al.* Wilkes subglacial basin ice sheet response to Southern Ocean warming during late Pleistocene interglacials. *Nat. Commun.* **13**, 5328 (2022).

125. Blackburn, T. *et al.* Ice retreat in Wilkes Basin of East Antarctica during a warm interglacial. *Nature* **583**, 554–559 (2020).

126. Edwards, T. L. *et al.* Projected land ice contributions to twenty-first-century sea level rise. *Nature* **593**, 74–82 (2021).

127. Dunmire, D., Lenaerts, J. T. M., Datta, R. T. & Gorte, T. Antarctic surface climate and surface mass balance in the Community Earth System Model version 2 during the satellite era and into the future (1979–2100). *Cryosphere* **16**, 4163–4184 (2022).

128. DeConto, R. M. & Pollard, D. Contribution of Antarctica to past and future sea-level rise. *Nature* **531**, 591–597 (2016).

129. Jourdain, N. C., Mathiot, P., Burgard, C., Caillet, J. & Kittel, C. Ice shelf basal melt rates in the Amundsen Sea at the end of the 21st century. Preprint at https://doi.org/10.1002/essoar.10511482.2.

130. Golledge, N. R. *et al.* Global environmental consequences of twenty-first-century ice-sheet melt. *Nature* **566**, 65–72 (2019).

131. Hellmer, H. H., Kauker, F., Timmermann, R., Determann, J. & Rae, J. Twenty-first-century warming of a large Antarctic ice-shelf cavity by a redirected coastal current. *Nature* **485**, 225–228 (2012).

132. Hellmer, H. H., Kauker, F., Timmermann, R. & Hattermann, T. The Fate of the Southern Weddell Sea Continental Shelf in a Warming Climate. *Journal of Climate* vol. 30 4337–4350 Preprint at https://doi.org/10.1175/jcli-d-16-0420.1 (2017).

133. Naughten, K. A. *et al.* Two-timescale response of a large Antarctic ice shelf to climate change. *Nature Communications* vol. 12 Preprint at https://doi.org/10.1038/s41467-021-22259-0 (2021).

134. Christianson, K. *et al.* Sensitivity of Pine Island Glacier to observed ocean forcing. *Geophysical Research Letters* vol. 43 Preprint at https://doi.org/10.1002/2016gl070500 (2016).

135. Milillo, P. *et al.* Rapid glacier retreat rates observed in West Antarctica. *Nature Geoscience* vol. 15 48–53 Preprint at https://doi.org/10.1038/s41561-021-00877-z

(2022).

136. Goldberg, D. N. *et al.* Representing grounding line migration in synchronous coupling between a marine ice sheet model and a z-coordinate ocean model. *Ocean Modelling* vol. 125 45–60 Preprint at https://doi.org/10.1016/j.ocemod.2018.03.005 (2018).

137. De Rydt, J., De Rydt, J. & Gudmundsson, G. H. Coupled ice shelf-ocean modeling and complex grounding line retreat from a seabed ridge. *Journal of Geophysical Research: Earth Surface* vol. 121 865–880 Preprint at https://doi.org/10.1002/2015jf003791 (2016).

138. Seroussi, H. *et al.* ISMIP6 Antarctica: a multi-model ensemble of the Antarctic ice sheet evolution over the 21st century. *The Cryosphere* vol. 14 3033–3070 Preprint at https://doi.org/10.5194/tc-14-3033-2020 (2020).

139. Bart, P. J., DeCesare, M., Rosenheim, B. E., Majewski, W. & McGlannan, A. A centuries-long delay between a paleo-ice-shelf collapse and grounding-line retreat in the Whales Deep Basin, eastern Ross Sea, Antarctica. *Sci. Rep.* **8**, 12392 (2018).

140. Jamieson, S. S. R. *et al.* Ice-stream stability on a reverse bed slope. *Nature Geoscience* vol. 5 799–802 Preprint at https://doi.org/10.1038/ngeo1600 (2012).

141. Alley, R. B., Anandakrishnan, S., Dupont, T. K., Parizek, B. R. & Pollard, D. Effect of sedimentation on ice-sheet grounding-line stability. *Science* **315**, 1838–1841 (2007).

142. Horgan, H. J., Christianson, K., Jacobel, R. W., Anandakrishnan, S. & Alley, R. B. Sediment deposition at the modern grounding zone of Whillans Ice Stream, West Antarctica. *Geophysical Research Letters* vol. 40 3934–3939 Preprint at https://doi.org/10.1002/grl.50712 (2013).

143. Kingslake, J., Ely, J. C., Das, I. & Bell, R. E. Widespread movement of meltwater onto and across Antarctic ice shelves. *Nature* **544**, 349–352 (2017).

144. Dutrieux, P. *et al.* Strong sensitivity of Pine Island ice-shelf melting to climatic variability. *Science* **343**, 174–178 (2014).

145. Smith, J. A. *et al.* Sub-ice-shelf sediments record history of twentieth-century retreat of Pine Island Glacier. *Nature* **541**, 77–80 (2017).

146. Holland, P. R., Bracegirdle, T. J., Dutrieux, P., Jenkins, A. & Steig, E. J. West Antarctic ice loss influenced by internal climate variability and anthropogenic forcing. *Nat. Geosci.* **12**, 718–724 (2019).

147. Holland, P. R. *et al.* Anthropogenic and internal drivers of wind changes over the Amundsen Sea, West Antarctica, during the 20th and 21st centuries. *The Cryosphere* **16**, 5085–5105 (2022).

148. Dowdeswell, J. A. *et al.* Delicate seafloor landforms reveal past Antarctic grounding-line retreat of kilometers per year. *Science* **368**, 1020–1024 (2020).

149. Graham, A. G. C. *et al.* Rapid retreat of Thwaites Glacier in the pre-satellite era. *Nature Geoscience* vol. 15 706–713 Preprint at https://doi.org/10.1038/s41561-022-01019-9 (2022).

150. Batchelor, C. L. *et al.* Rapid, buoyancy-driven ice-sheet retreat of hundreds of metres per day. *Nature* **617**, 105–110 (2023).

151. Tedesco, M. & Fettweis, X. Unprecedented atmospheric conditions (1948–2019) drive the 2019 exceptional melting season over the Greenland ice sheet. *cryosphere* **14**, 1209–1223 (2020).

152. Moon, T. A. NOAA arctic report card 2022: Greenland ice sheet. (2022) doi:10.25923/C430-HB50.

153. Otosaka, I. N. *et al.* Mass balance of the Greenland and Antarctic ice sheets from 1992 to 2020. *Earth Syst. Sci. Data* **15**, 1597–1616 (2023).

154. Mattingly, K. S., Mote, T. L. & Fettweis, X. Atmospheric river impacts on Greenland ice sheet surface mass balance. *J. Geophys. Res.* **123**, 8538–8560 (2018).

155. Mattingly, K. S., Ramseyer, C. A., Rosen, J. J., Mote, T. L. & Muthyala, R. Increasing water vapor transport to the Greenland Ice Sheet revealed using self-organizing maps: INCREASING GREENLAND MOISTURE TRANSPORT. *Geophys. Res. Lett.* **43**, 9250–9258 (2016).

156. Box, J. E. *et al.* Greenland ice sheet rainfall, heat and albedo feedback impacts from the mid-august 2021 atmospheric river. *Geophys. Res. Lett.* **49**, (2022).

157. Hanna, E. *et al.* Greenland surface air temperature changes from 1981 to 2019 and implications for ice-sheet melt and mass-balance change. *Int. J. Climatol.* **41**, (2021).

158. Niwano, M. *et al.* Rainfall on the Greenland ice sheet: present-day climatology from a high-resolution non-hydrostatic polar regional climate model. *Geophys. Res. Lett.* (2021).

159. Bartholomew, I. D. *et al.* Seasonal variations in Greenland Ice Sheet motion: Inland extent and behaviour at higher elevations. *Earth Planet. Sci. Lett.* **307**, 271–278 (2011).

160. Rathmann, N. M. *et al.* Highly temporally resolved response to seasonal surface melt of the Zachariae and 79N outlet glaciers in northeast Greenland. *Geophys. Res. Lett.* **44**, 9805–9814 (2017).

161. Larsen, S. H. *et al.* Outlet glacier flow response to surface melt: based on analysis of a high-resolution satellite data set. *J. Glaciol.* 1–9 (2023).

162. Moon, T. *et al.* Distinct patterns of seasonal Greenland glacier velocity. *Geophys. Res. Lett.* **41**, 7209–7216 (2014).

163. Stevens, L. A. *et al.* Tidewater-glacier response to supraglacial lake drainage. *Nat. Commun.* **13**, 6065 (2022).

164. Solgaard, A. M., D., R., Noël & Hvidberg, C. S. Seasonal patterns of Greenland ice velocity from Sentinel-1 SAR data linked to runoff. *Geophys. Res. Lett.* (2022).

165. Nettles, M. *et al.* Step-wise changes in glacier flow speed coincide with calving and glacial earthquakes at Helheim Glacier, Greenland. *Geophys. Res. Lett.* **35**, L24503 (2008).

166. Cassotto, R. *et al.* Non-linear glacier response to calving events, Jakobshavn Isbræ, Greenland. *J. Glaciol.* **65**, 39–54 (2019).

167. Amundson, J. M., Truffer, M. & Zwinger, T. Tidewater glacier response to individual calving events. *J. Glaciol.* **68**, 1117–1126 (2022).

168. Khan, S.A., Wahr, J., Bevis, M., Velicogna, I, Kendrick, E. Spread of ice mass loss into northwest Greenland observed by GRACE and GPS. *Geophys. Res. Lett.* 37 (6), doi:10.1029/2010GL042460 (2010).

169. Catania, G. A. *et al.* Geometric controls on tidewater glacier retreat in central western Greenland. *J. Geophys. Res. Earth Surf.* **123**, 2024–2038 (2018).

170. Enderlin, E. M., Howat, I. M. & Vieli, A. High sensitivity of tidewater outlet glacier dynamics to shape. *The Cryosphere* **7**, 1007–1015 (2013).

171. de Juan, J. *et al.* Sudden increase in tidal response linked to calving and acceleration at a large Greenland outlet glacier. *Geophys. Res. Lett.* **37**, (2010).

172. van Dongen, E. *et al.* Tides modulate crevasse opening prior to a major calving event at Bowdoin Glacier, Northwest Greenland. *J. Glaciol.* **66**, 113–123 (2020).

173. Ma, Y. & Bassis, J. N. The Effect of Submarine Melting on Calving From Marine Terminating Glaciers. *J. Geophys. Res.* **124**, 334–346 (2019).

174. van Dongen, E. C. H. *et al.* Numerical Modeling Shows Increased Fracturing Due to Melt-Undercutting Prior to Major Calving at Bowdoin Glacier. *Front Earth Sci. Chin.* **8**,

(2020).

175. Chauché, N., Hubbard, A., Gascard, J. C. & Box, J. E. Ice–ocean interaction and calving front morphology at two west Greenland tidewater outlet glaciers. *The* (2014).

176. Cassotto, R., Fahnestock, M., Amundson, J. M., Truffer, M. & Joughin, I. Seasonal and interannual variations in ice melange and its impact on terminus stability, Jakobshavn Isbræ, Greenland. *J. Glaciol.* **61**, 76–88 (2015).

177. Moon, T., Joughin, I. & Smith, B. Seasonal to multiyear variability of glacier surface velocity, terminus position, and sea ice/ice mélange in northwest Greenland. *J. Geophys. Res.* **120**, 818–833 (2015).

178. Cook, S. *et al.* Modelling environmental influences on calving at Helheim Glacier in eastern Greenland. *Cryosphere* **8**, 827–841 (2014).

179. Box, J. E. *et al.* Greenland ice sheet climate disequilibrium and committed sea-level rise. *Nature Climate Change* vol. 12 808–813 Preprint at https://doi.org/10.1038/s41558-022-01441-2 (2022).

180. Fettweis, X. *et al.* GrSMBMIP: Intercomparison of the modelled 1980–2012 surface mass balance over the Greenland Ice sheet. Preprint at https://doi.org/10.5194/tc-2019-321.

181. Trusel, L. D. *et al.* Nonlinear rise in Greenland runoff in response to post-industrial Arctic warming. *Nature* **564**, 104–108 (2018).

182. Box, J. E. *et al.* Greenland ice sheet mass balance reconstruction. Part I: Net snow accumulation (1600–2009). *Journal of Climate* **26**, (2013).

183. MacFerrin, M. *et al.* Rapid expansion of Greenland's low-permeability ice slabs. *Nature* **573**, 403–407 (2019).

184. Culberg, R., Schroeder, D. M. & Chu, W. Extreme melt season ice layers reduce firn

permeability across Greenland. *Nat. Commun.* **12**, 1–9 (2021).

185. Tedstone, A. J. & Machguth, H. Increasing surface runoff from Greenland's firn areas. *Nat. Clim. Chang.* **12**, 672–676 (2022).

186. Ryan, J. C. *et al.* Greenland Ice Sheet surface melt amplified by snowline migration and bare ice exposure. *Sci Adv* **5**, eaav3738 (2019).

187. Horlings, A. N., Christianson, K. & Miège, C. Expansion of Firn Aquifers in Southeast Greenland. *J. Geophys. Res.* **127**, e2022JF006753 (2022).

188. NEEM community members. Eemian interglacial reconstructed from a Greenland folded ice core. *Nature* vol. 493 489–494 (2013).

189. Vinther, B. M. *et al.* Holocene thinning of the Greenland ice sheet. *Nature* **461**, 385–388 (2009).

190. Sasgen, I. *et al.* Return to rapid ice loss in Greenland and record loss in 2019 detected by the GRACE-FO satellites. *Communications Earth & Environment* vol. 1 Preprint at https://doi.org/10.1038/s43247-020-0010-1 (2020).

191. Mankoff, K. D. *et al.* Greenland ice sheet mass balance from 1840 through next week. *Earth Syst. Sci. Data* **13**, 5001–5025 (2021).

192. Fettweis, X. *et al.* Reconstructions of the 1900–2015 Greenland ice sheet surface mass balance using the regional climate MAR model. *The Cryosphere* vol. 11 1015–1033 Preprint at https://doi.org/10.5194/tc-11-1015-2017 (2017).

193. Noël, B., Lenaerts, J. T. M., Lipscomb, W. H., Thayer-Calder, K. & van den Broeke, M. R. Peak refreezing in the Greenland firn layer under future warming scenarios. *Nat. Commun.* **13**, 1–10 (2022).

194. Noël, B., van Kampenhout, L., Lenaerts, J. T. M., van de Berg, W. J. & van den Broeke, M. R. A 21st century warming threshold for sustained Greenland ice sheet mass loss.

Geophys. Res. Lett. **48**, (2021).

195. clec'h, S. L. *et al.* Assessment of the Greenland ice sheet–atmosphere feedbacks for the next century with a regional atmospheric model coupled to an ice sheet model. *The Cryosphere* vol. 13 373–395 Preprint at https://doi.org/10.5194/tc-13-373-2019 (2019).
196. Boberg, F., Mottram, R., Hansen, N., Yang, S. & Langen, P. L. Uncertainties in projected surface mass balance over the polar ice sheets from dynamically downscaled EC-Earth models. *Cryosphere* **16**, 17–33 (2022).
197. Robinson, A., Calov, R. & Ganopolski, A. Multistability and critical thresholds of the Greenland ice sheet. *Nat. Clim. Chang.* (2012).
198. Aschwanden, A. *et al.* Contribution of the Greenland Ice Sheet to sea level over the next millennium. *Sci Adv* **5**, eaav9396 (2019).
199. Gregory, J. M., George, S. E. & Smith, R. S. Large and irreversible future decline of the Greenland ice sheet. *The Cryosphere* **14**, 4299–4322 (2020).
200. Holland, D. M., Thomas, R. H., de Young, B., Ribergaard, M. H. & Lyberth, B. Acceleration of Jakobshavn Isbræ triggered by warm subsurface ocean waters. *Nat. Geosci.* **1**, 659–664 (2008).
201. Slater, D. A. & Straneo, F. Submarine melting of glaciers in Greenland amplified by atmospheric warming. *Nat. Geosci.* **15**, 794–799 (2022).
202. Ultee, L., Felikson, D., Minchew, B., Stearns, L. A. & Riel, B. Helheim Glacier ice velocity variability responds to runoff and terminus position change at different timescales. *Nat. Commun.* **13**, 1–10 (2022).
203. Barnett, J., Holmes, F. A. & Kirchner, N. Modelled dynamic retreat of Kangerlussuaq Glacier, East Greenland, strongly influenced by the consecutive absence of an ice mélange in Kangerlussuaq Fjord. *J. Glaciol.* 1–12 (2022).

204. Christian, J. E. *et al.* The contrasting response of outlet glaciers to interior and ocean forcing. *The Cryosphere* **14**, 2515–2535 (2020).

205. Grinsted, A. *et al.* Accelerating ice flow at the onset of the Northeast Greenland Ice Stream. *Nat. Commun.* **13**, 1–4 (2022).

206. Zwally, H. J. *et al.* Surface melt-induced acceleration of Greenland ice-sheet flow. *Science* **297**, 218–222 (2002).

207. Wal, R. S. W. van de *et al.* Self-regulation of ice flow varies across the ablation area in south-west Greenland. *The Cryosphere* vol. 9 603–611 Preprint at https://doi.org/10.5194/tc-9-603-2015 (2015).

208. Tedstone, A. J. *et al.* Decadal slowdown of a land-terminating sector of the Greenland Ice Sheet despite warming. *Nature* **526**, 692–695 (2015).

209. Sole, A. *et al.* Winter motion mediates dynamic response of the Greenland Ice Sheet to warmer summers. *Geophys. Res. Lett.* **40**, 3940–3944 (2013).

210. Andersen, M. L. *et al.* Quantitative estimates of velocity sensitivity to surface melt variations at a large Greenland outlet glacier. *J. Glaciol.* **57**, 609–620 (2011).

211. Nienow, P. W., Sole, A. J., Slater, D. A. & Cowton, T. R. Recent Advances in Our Understanding of the Role of Meltwater in the Greenland Ice Sheet System. *Current Climate Change Reports* **3**, 330–344 (2017).

212. Doyle, S. H. *et al.* Persistent flow acceleration within the interior of the Greenland ice sheet. *Geophys. Res. Lett.* **41**, 899–905 (2014).

213. Clason, C. C. *et al.* Modelling the transfer of supraglacial meltwater to the bed of Leverett Glacier, Southwest Greenland. *The Cryosphere* vol. 9 123–138 Preprint at https://doi.org/10.5194/tc-9-123-2015 (2015).

214. Doyle, S. H. *et al.* Amplified melt and flow of the Greenland ice sheet driven by late-

summer cyclonic rainfall. *Nature Geoscience* vol. 8 647–653 Preprint at https://doi.org/10.1038/ngeo2482 (2015).

215. Rignot, E. & Kanagaratnam, P. Changes in the velocity structure of the Greenland Ice Sheet. *Science* **311**, 986–990 (2006).

216. Bassis, J. N. The statistical physics of iceberg calving and the emergence of universal calving laws. *J. Glaciol.* **57**, 3–16 (2011).

217. Luckman, A., Murray, T., de Lange, R. & Hanna, E. Rapid and synchronous ice-dynamic changes in East Greenland. *Geophys. Res. Lett.* **33**, (2006).

218. Csatho, B., Schenk, T., Van Der Veen, C. J. & Krabill, W. B. Intermittent thinning of Jakobshavn Isbræ, West Greenland, since the Little Ice Age. *J. Glaciol.* **54**, 131–144 (2008).

219. Nick, F. M., Vieli, A., Howat, I. M. & Joughin, I. Large-scale changes in Greenland outlet glacier dynamics triggered at the terminus. *Nat. Geosci.* **2**, 110–114 (2009).

220. Felikson, D. *et al.* Inland thinning on the Greenland ice sheet controlled by outlet glacier geometry. *Nat. Geosci.* **10**, 366–369 (2017).

221. Khan, S. A. *et al.* Extensive inland thinning and speed-up of Northeast Greenland Ice Stream. *Nature* **611**, 727–732 (2022).

222. Kehrl, L. M., Joughin, I., Shean, D. E., Floricioiu, D. & Krieger, L. Seasonal and interannual variabilities in terminus position, glacier velocity, and surface elevation at Helheim and Kangerlussuaq Glaciers from 2008 to 2016. *J. Geophys. Res.* **122**, 1635–1652 (2017).

223. Robel, A. A., Seroussi, H. & Roe, G. H. Marine ice sheet instability amplifies and skews uncertainty in projections of future sea-level rise. *Proceedings of the National Academy of Sciences* **116**, 14887–14892 (2019).

224. Felikson, D., Nowicki, S., Nias, I., Morlighem, M. & Seroussi, H. Seasonal Tidewater Glacier Terminus Oscillations Bias Multi-Decadal Projections of Ice Mass Change. *J. Geophys. Res.* **127**, e2021JF006249 (2022).

225. Tapley, B. D. *et al.* Contributions of GRACE to understanding climate change. *Nat. Clim. Chang.* **5**, 358–369 (2019).

226. Rees, E. R. *et al.* Absolute frequency readout derived from ULE cavity for next generation geodesy missions. *Optics Express* vol. 29 26014 Preprint at https://doi.org/10.1364/oe.434483 (2021).

227. Flechtner, F. *et al.* What Can be Expected from the GRACE-FO Laser Ranging Interferometer for Earth Science Applications? *Surveys in Geophysics* vol. 37 453–470 Preprint at https://doi.org/10.1007/s10712-015-9338-y (2016).

228. [No title]. https://www.asi.it/wp-content/uploads/2021/03/MAGIC_NGGM_MCDO_MRD_v1_0-signed2.pdf.

229. Davis, P. E. D. *et al.* Suppressed basal melting in the eastern Thwaites Glacier grounding zone. *Nature* **614**, 479–485 (2023).

230. Schmidt, B. E. *et al.* Heterogeneous melting near the Thwaites Glacier grounding line. *Nature* **614**, 471–478 (2023).

231. Vaňková, I. & Nicholls, K. W. Ocean Variability Beneath the Filchner-Ronne Ice Shelf Inferred From Basal Melt Rate Time Series. *Journal of Geophysical Research: Oceans* vol. 127 Preprint at https://doi.org/10.1029/2022jc018879 (2022).

232. Sutherland, D. A. *et al.* Direct observations of submarine melt and subsurface geometry at a tidewater glacier. *Science* **365**, 369–374 (2019).

233. Morlighem, M. *et al.* Deep glacial troughs and stabilizing ridges unveiled beneath the margins of the Antarctic ice sheet. *Nat. Geosci.* **13**, 132–137 (2020).

234. Colleoni, F. *et al.* Spatio-temporal variability of processes across Antarctic ice-bed-ocean interfaces. *Nat. Commun.* **9**, 2289 (2018).

235. Zheng, L. *et al.* Greenland Ice Sheet Daily Surface Melt Flux Observed From Space. *Geophysical Research Letters* vol. 49 Preprint at https://doi.org/10.1029/2021gl096690 (2022).

236. Banwell, A. F., Willis, I. C., Macdonald, G. J., Goodsell, B. & MacAyeal, D. R. Direct measurements of ice-shelf flexure caused by surface meltwater ponding and drainage. *Nat. Commun.* **10**, 730 (2019).

237. Stibal, M. *et al.* Algae drive enhanced darkening of bare ice on the Greenland ice sheet. *Geophys. Res. Lett.* **44**, 11,463–11,471 (2017).

238. Khazendar, A. *et al.* Author Correction: Interruption of two decades of Jakobshavn Isbrae acceleration and thinning as regional ocean cools. *Nat. Geosci.* **12**, 493–493 (2019).

239. Truffer, M. & Fahnestock, M. CLIMATE CHANGE: Rethinking Ice Sheet Time Scales. *Science* vol. 315 1508–1510 Preprint at https://doi.org/10.1126/science.1140469 (2007).

240. Mouginot, J. *et al.* Fast retreat of Zachariæ Isstrøm, northeast Greenland. *Science* **350**, 1357–1361 (2015).

241. Phillips, T., Rajaram, H. & Steffen, K. Cryo-hydrologic warming: A potential mechanism for rapid thermal response of ice sheets. *Geophysical Research Letters* vol. 37 Preprint at https://doi.org/10.1029/2010gl044397 (2010).

242. van de Wal, R. S. W. *et al.* A high-end estimate of sea level rise for practitioners. *Earths Future* **10**, e2022EF002751 (2022).

243. Fettweis, X. *et al. Brief communication* 'Important role of the mid-tropospheric

atmospheric circulation in the recent surface melt increase over the Greenland ice sheet'. *The Cryosphere* vol. 7 241–248 Preprint at https://doi.org/10.5194/tc-7-241-2013 (2013).

244. Topál, D. *et al.* Discrepancies between observations and climate models of large-scale wind-driven Greenland melt influence sea-level rise projections. *Nat. Commun.* **13**, 6833 (2022).

245. Delhasse, A., Fettweis, X., Kittel, C., Amory, C. & Agosta, C. Brief communication: Impact of the recent atmospheric circulation change in summer on the future surface mass balance of the Greenland Ice Sheet. *The Cryosphere* vol. 12 3409–3418 Preprint at https://doi.org/10.5194/tc-12-3409-2018 (2018).

246. Benn, D. I., Cowton, T., Todd, J. & Luckman, A. Glacier Calving in Greenland. *Current Climate Change Reports* **3**, 282–290 (2017).

247. Sun, S., Cornford, S. L., Moore, J. C., Gladstone, R. & Zhao, L. Ice shelf fracture parameterization in an ice sheet model. *The Cryosphere* vol. 11 2543–2554 Preprint at https://doi.org/10.5194/tc-11-2543-2017 (2017).

248. Krug, J., Weiss, J., Gagliardini, O. & Durand, G. Combining damage and fracture mechanics to model calving. *The Cryosphere* vol. 8 2101–2117 Preprint at https://doi.org/10.5194/tc-8-2101-2014 (2014).

249. Smith, R. S. *et al.* Coupling the U.K. Earth System Model to Dynamic Models of the Greenland and Antarctic Ice Sheets. *Journal of Advances in Modeling Earth Systems* vol. 13 Preprint at https://doi.org/10.1029/2021ms002520 (2021).

250. Bradley, A. T., Bett, D. T., Dutrieux, P., De Rydt, J. & Holland, P. R. The Influence of Pine Island Ice Shelf Calving on Basal Melting. *Journal of Geophysical Research: Oceans* vol. 127 Preprint at https://doi.org/10.1029/2022jc018621 (2022).

251. Reese, R., Levermann, A., Albrecht, T., Seroussi, H. & Winkelmann, R. The role of history and strength of the oceanic forcing in sea level projections from Antarctica with the Parallel Ice Sheet Model. *The Cryosphere* vol. 14 3097–3110 Preprint at https://doi.org/10.5194/tc-14-3097-2020 (2020).

252. Jourdain, N. C. *et al.* A protocol for calculating basal melt rates in the ISMIP6 Antarctic ice sheet projections. *The Cryosphere* vol. 14 3111–3134 Preprint at https://doi.org/10.5194/tc-14-3111-2020 (2020).

253. Burgard, C., Jourdain, N. C., Reese, R., Jenkins, A. & Mathiot, P. An assessment of basal melt parameterisations for Antarctic ice shelves. *The Cryosphere* vol. 16 4931–4975 Preprint at https://doi.org/10.5194/tc-16-4931-2022 (2022).

254. Muntjewerf, L. *et al.* Description and Demonstration of the Coupled Community Earth System Model v2 - Community Ice Sheet Model v2 (CESM2-CISM2). *J Adv Model Earth Syst* **13**, e2020MS002356 (2021).

255. Siahaan, A. *et al.* The Antarctic contribution to 21st-century sea-level rise predicted by the UK Earth System Model with an interactive ice sheet. *The Cryosphere* **16**, 4053–4086 (2022).

256. Ivins, E. R. *et al.* Antarctic contribution to sea level rise observed by GRACE with improved GIA correction. *Journal of Geophysical Research: Solid Earth* vol. 118 3126–3141 Preprint at https://doi.org/10.1002/jgrb.50208 (2013).

257. Sasgen, I. *et al.* Antarctic ice-mass balance 2003 to 2012: regional reanalysis of GRACE satellite gravimetry measurements with improved estimate of glacial-isostatic adjustment based on GPS uplift rates. *The Cryosphere* vol. 7 1499–1512 Preprint at https://doi.org/10.5194/tc-7-1499-2013 (2013).

258. Peltier, W. R., Argus, D. F. & Drummond, R. Space geodesy constrains ice age terminal

deglaciation: The global ICE-6G_C (VM5a) model. *Journal of Geophysical Research: Solid Earth* vol. 120 450–487 Preprint at https://doi.org/10.1002/2014jb011176 (2015).

259. Diener, T. *et al.* Acceleration of Dynamic Ice Loss in Antarctica From Satellite Gravimetry. *Frontiers in Earth Science* vol. 9 Preprint at https://doi.org/10.3389/feart.2021.741789 (2021).

260. Khan, S. A. *et al.* Geodetic measurements reveal similarities between post-Last Glacial Maximum and present-day mass loss from the Greenland ice sheet. *Sci Adv* **2**, e1600931 (2016).

261. McKay, R. M. *et al.* Cenozoic history of Antarctic glaciation and climate from onshore and offshore studies. *Antarctic Climate Evolution* 41–164 Preprint at https://doi.org/10.1016/b978-0-12-819109-5.00008-6 (2022).

262. Dorschel, B. *et al.* The International Bathymetric Chart of the Southern Ocean Version 2. *Sci Data* **9**, 275 (2022).

263. Eyring, V. *et al.* Overview of the Coupled Model Intercomparison Project Phase 6 (CMIP6) experimental design and organization. *Geosci. Model Dev.* **9**, 1937–1958 (2016).

264. Box, J. E. *et al.* Greenland ice sheet rainfall climatology, extremes and atmospheric river rapids. *Meteorol. Appl.*

265. Bart, P. J., DeCesare, M., Rosenheim, B. E., Majewski, W. & McGlannan, A. A centuries-long delay between a paleo-ice-shelf collapse and grounding-line retreat in the Whales Deep Basin, eastern Ross Sea, Antarctica. *Sci. Rep.* **8**, 12392 (2018).

266. Jamieson, S. S. R. *et al.* Ice-stream stability on a reverse bed slope. *Nature Geoscience* vol. 5 799–802 Preprint at https://doi.org/10.1038/ngeo1600 (2012).

267. Dowdeswell, J. A. *et al.* Delicate seafloor landforms reveal past Antarctic grounding-line

retreat of kilometers per year. *Science* **368**, 1020–1024 (2020).
268. Graham, A. G. C. *et al.* Rapid retreat of Thwaites Glacier in the pre-satellite era. *Nature Geoscience* vol. 15 706–713 Preprint at https://doi.org/10.1038/s41561-022-01019-9 (2022).
269. Barletta, V. R. *et al.* Observed rapid bedrock uplift in Amundsen Sea Embayment promotes ice-sheet stability. *Science* **360**, 1335–1339 (2018).
270. Whitehouse, P. L. Glacial isostatic adjustment modelling: historical perspectives, recent advances, and future directions. *Earth Surf. Dyn.* **6**, 401–429 (2018).
271. Pollard, D., DeConto, R. M. & Alley, R. B. Potential Antarctic Ice Sheet retreat driven by hydrofracturing and ice cliff failure. *Earth and Planetary Science Letters* vol. 412 112–121 Preprint at https://doi.org/10.1016/j.epsl.2014.12.035 (2015).

Acknowledgements. We are grateful to the World Climate Research Programme's Climate & Cryosphere core project, the International Arctic Science Committee and SCAR for co-sponsoring an ISMASS workshop that led to this collaboration. E.H. and A.S. acknowledge funding from NERC (NE/W005875/1 and NE/V014285/1). F.D.W.C. acknowledges funding from the Prince Albert II of Monaco Foundation. This work is part of the TiPACCs project, which receives funding from the European Union's Horizon 2020 research and innovation programme under grant agreement no. 820575. H.G. received funding from the EU's Horizon 2020 Research and Innovation Programme under grant agreement no. 869304, PROTECT and from the Research Council of Norway under projects 295046 and 324639. L.D. acknowledges funding from the PNRA19_00022 project. F.Col. acknowledges funding from the PNRA18_00002 project and from the SCAR INSTANT Programme. R.M. acknowledges the support of the Danish state via the National Centre for Klima Forskning. I.S. acknowledges funding by the Helmholtz Climate Initiative REKLIM (Regional Climate Change), a joint research project of the Helmholtz Association of German Research Centres (HGF). We thank Pepsi Hanna for help with figure preparation. A.G. acknowledges financial support from the New Zealand Ministry for Business Innovation and Employment (grant no. ANTA1801; "Antarctic Science Platform").

Author contributions. E.H. designed and co-ordinated the study and raised critical funding support for the ISMASS workshop. E.H., J.B., S.B., F.D.W.C., C.H., M.M., D.T., L.D. and A.S. led the writing, and all authors contributed to the writing and discussion of ideas. I.S. designed Fig. 1, D.T. designed Figs. 2 & 5, F.Col. designed Fig. 3, and J.B. designed Fig. 4.

Competing interests. The authors declare no competing interests.

Figures

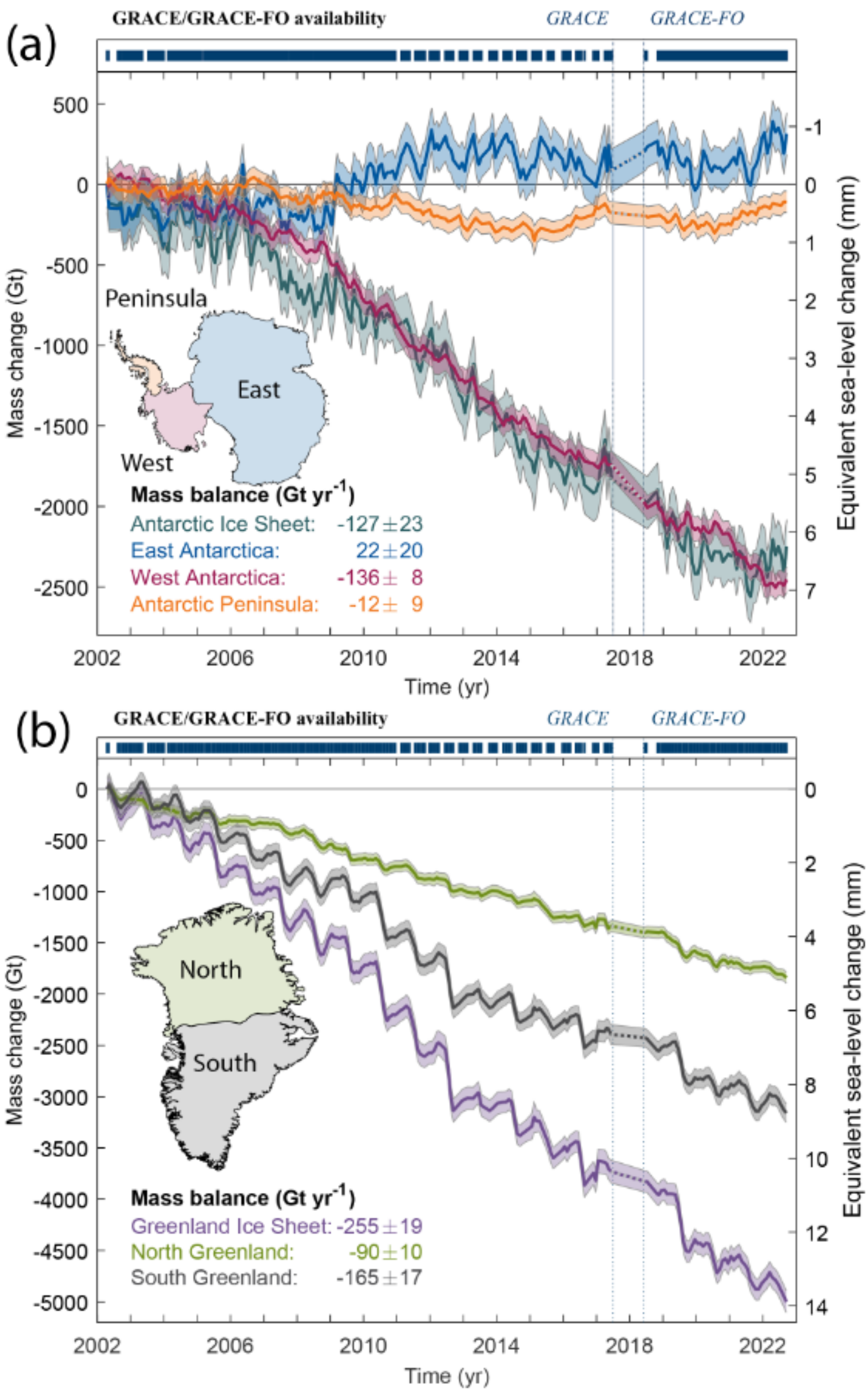
(a)
GRACE/GRACE-FO availability
GRACE
GRACE-FO
Mass change (Gt)
Equivalent sea-level change (mm)
Peninsula
East
West
Mass balance (Gt yr^{-1})
Antarctic Ice Sheet: -127±23
East Antarctica: 22±20
West Antarctica: -136± 8
Antarctic Peninsula: -12± 9
Time (yr)
(b)
GRACE/GRACE-FO availability
GRACE
GRACE-FO
Mass change (Gt)
Equivalent sea-level change (mm)
North
South
Mass balance (Gt yr^{-1})
Greenland Ice Sheet: -255±19
North Greenland: -90±10
South Greenland: -165±17
Time (yr)

Figure 1. Time series of mass change for (a) the Antarctic Ice Sheet and (b) the Greenland Ice Sheet for 2002 to 2022 based on 213 monthly gravity field solutions from GRACE/GRACE-FO satellite data. For Antarctica, estimates are shown for the entire ice sheet, as well as East Antarctica (blue), West Antarctica (red) and the Antarctic Peninsula (yellow). The glacial-isostatic adjustment (GIA) correction applied for Antarctica represents the arithmetic average of the models IJ05 R2[256], AGE1[257] and ICE-6G_D[258]; time series are updates from ref. 259. For Greenland, estimates are shown for the entire ice sheet (purple), as well as the regions north (green) and south (grey) of about 72°N. The correction for GIA is the GGG1.D model, tuned to fit measured GIA-induced GPS uplift rates[260]; time series are updates from ref. 190. Shading represents 2-sigma monthly empirical uncertainties. For the annotated mass balances, uncertainties consist of propagated empirical uncertainties and the spread of ten model corrections for GIA for Greenland[190] and thirteen for Antarctica[259]. Over the 21-year period Greenland lost approximately double the mass of Antarctica, while there are significant interannual variations in the mass changes of both ice sheets.

(a)

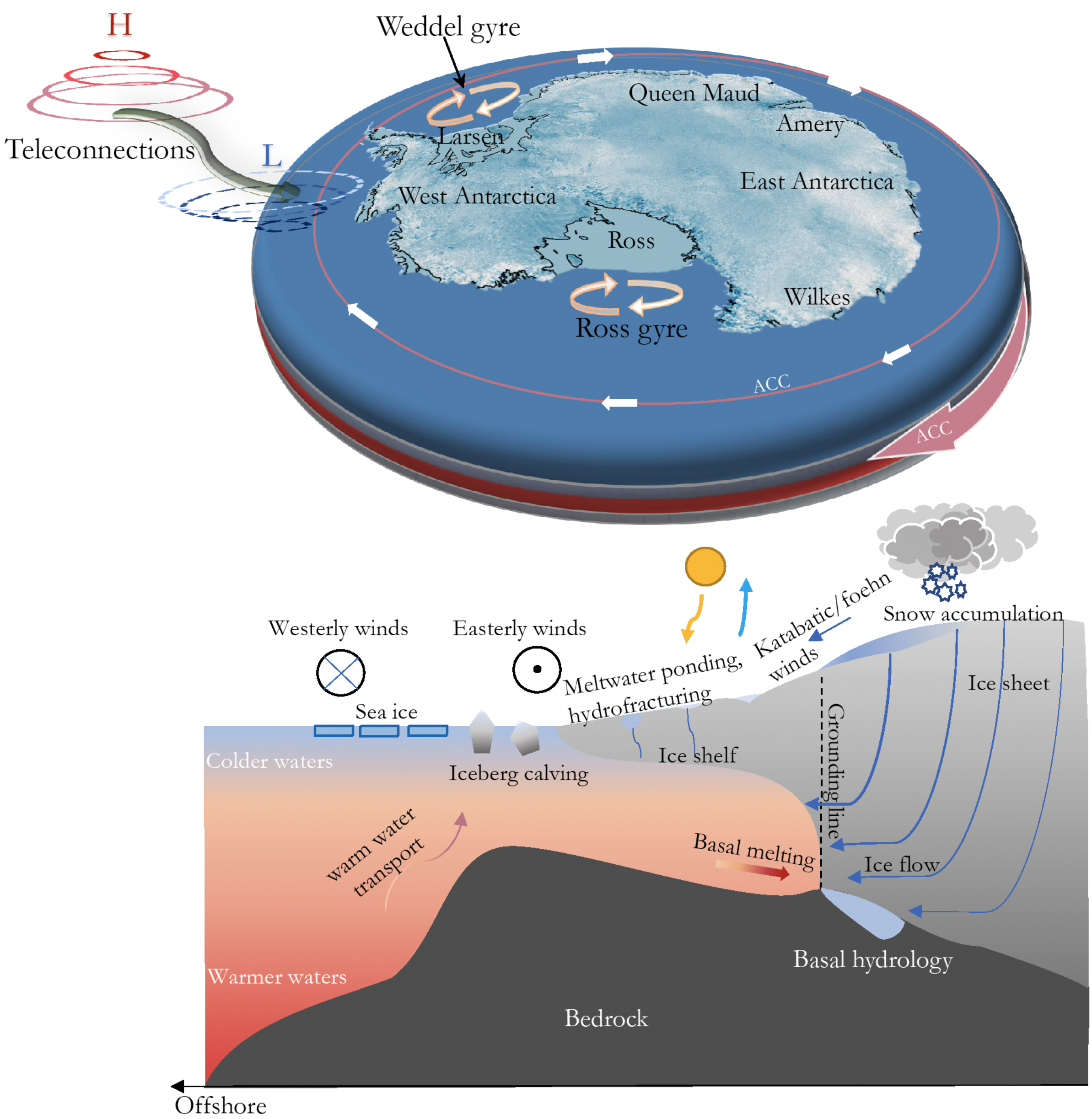
H
Weddel gyre
Teleconnections
L
Queen Maud
Amery
Larsen
West Antarctica
East Antarctica
Ross
Wilkes
Ross gyre
ACC
ACC
Westerly winds
Easterly winds
Meltwater ponding, hydrofracturing
Katabatic/foehn winds
Snow accumulation
Sea ice
Ice sheet
Colder waters
Iceberg calving
Ice shelf
Grounding line
warm water transport
Basal melting
Ice flow
Warmer waters
Basal hydrology
Bedrock
Offshore

(b)

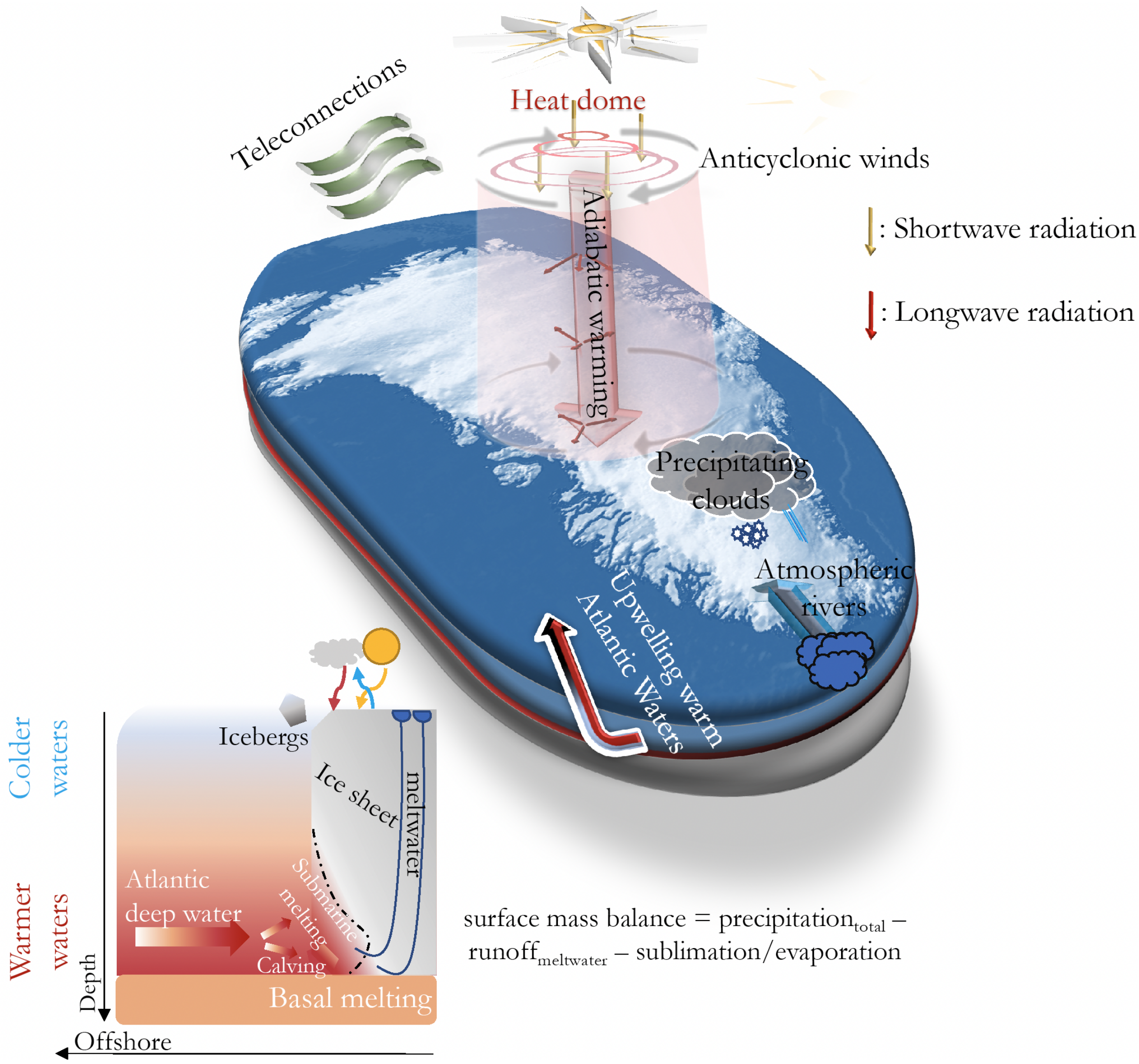

Figure 2. Schematic of key weather, climate, hydrological and ocean processes influencing (a) Antarctic and (b) Greenland ice-sheet mass balance. While Greenland is dominated by atmospheric processes, oceanic forcing predominates for the Antarctic Ice Sheet.

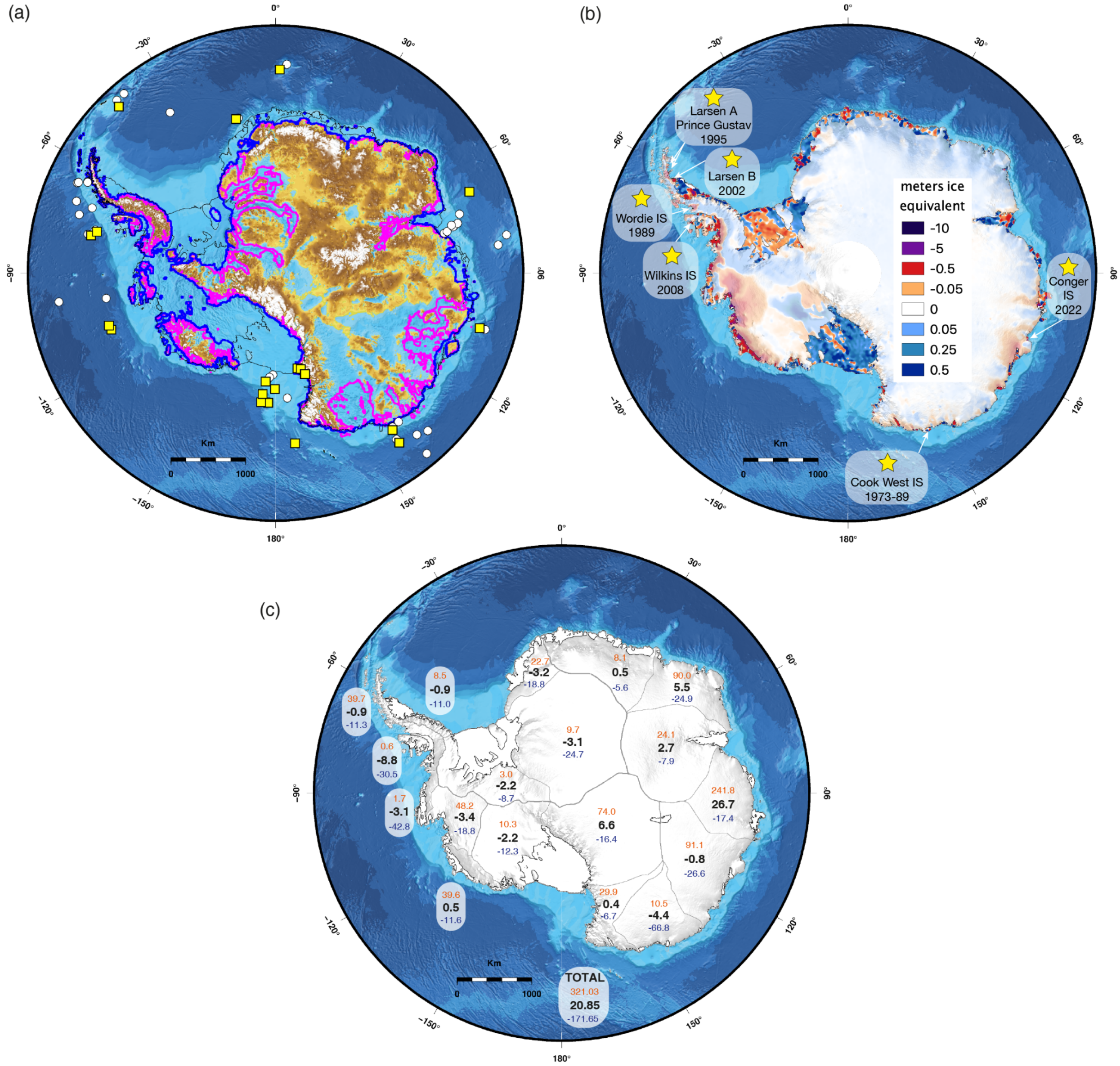

Figure 3. Past, present and future changes of the Antarctic Ice Sheet. (a) Simulated Antarctic ice sheet retreat during a generic warm interglacial of the Pliocene (magenta line) and during the Last great Interglacial (~130 ka, blue line, LIG) accounting for MICI[91]. White spots indicate all existing deep marine sediment drilling sites (Deep Sea Drilling Project, Ocean Drilling Program, International Ocean Discovery Program) around Antarctica and yellow squares correspond to the sites showing geological evidence for grounding-line retreat during the Pliocene and Pleistocene epochs[261]. (b) Antarctic ice thickness changes from 2003-2019[39]. Grounded ice thickness change is shown with semi-transparent colouring to emphasise rates of ice shelf-thinning. The locations of observed ice-shelf collapse events during the satellite era are also shown. (c) ISMIP6 ensemble member-derived volume changes above floatation in mm SLE in 2100 for emission scenario RCP8.5[138]. Changes are calculated relative to 2015

and using 362.5 Gt = 1 mm sea-level rise as a standard conversion factor (e.g. ref. 77), and positive values indicate a contribution to global mean sea-level rise. Numbers are shown for each drainage basin[23] and show the median (black), the min (blue) and the max (orange) from the ensemble. Overall, the ensemble indicates a maximum Antarctic contribution up to ~32 cm GMSR by 2100, in line with IPCC AR6 projections[2]. For panels (a) and (c), the black line corresponds to the present-day grounding line and coastline from BedMachine Antarctic v3[233]. Bathymetry is from IBCSO v2[262]. Knowledge of the AIS's past and ongoing behaviour is essential for accurately constraining projections of its future evolution.

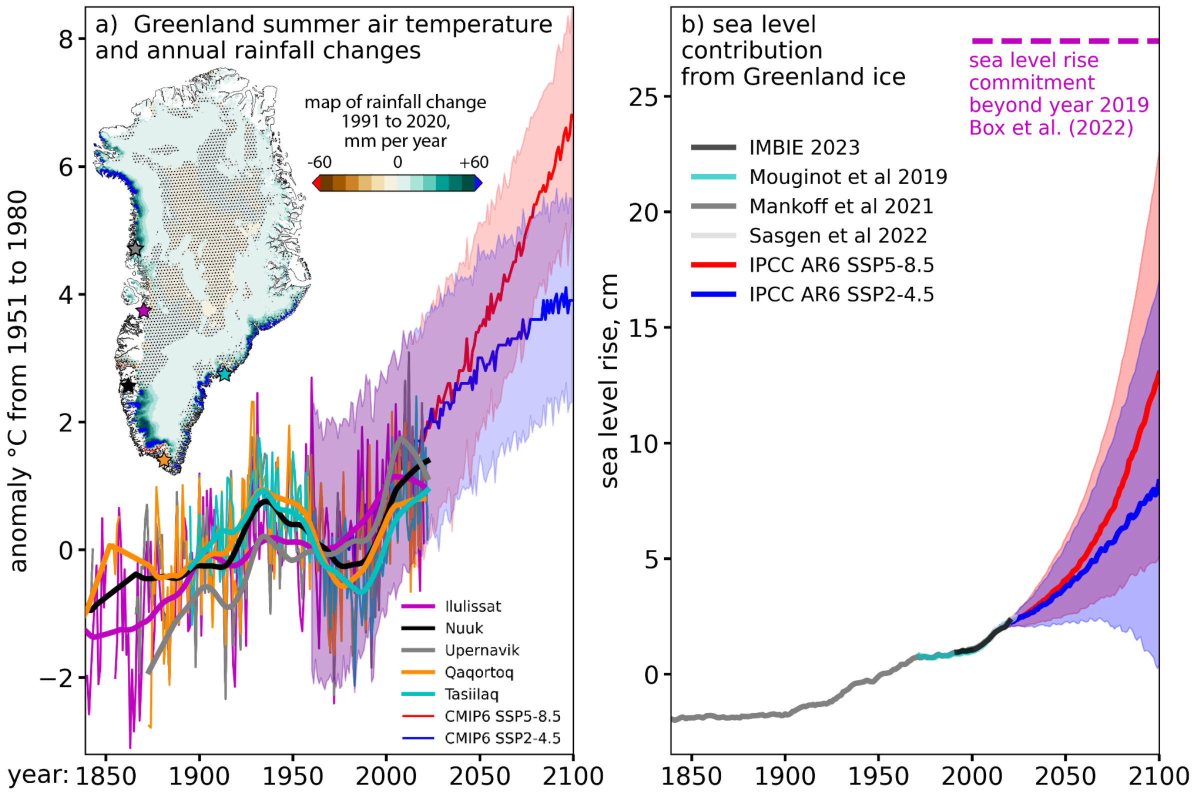

Figure 4. Past and future Greenland air temperature and sea-level contribution between 1850 and 2100. a) June through August summer air temperature data are from land-based observations (stations marked with asterisks) and projected from 1960 to 2100, data after ref. 263, courtesy of X. Fettweis. An inset rainfall trend map is derived from the Copernicus Arctic Regional ReAnalysis (CARRA)[264] on which non-stippled areas have trend confidence above 66% as measured as 1 minus the p-statistic, suggesting significant difference from a random series. No areas having rainfall decrease exceed 66% confidence. b) Greenland Ice Sheet mass balance sea-level equivalent (in cm). The observations and projections are offset to align with AR6 projections starting in 2016. The available data indicate that Greenland climate and the ice sheet sea level contribution has begun departing from a period of relative stability.

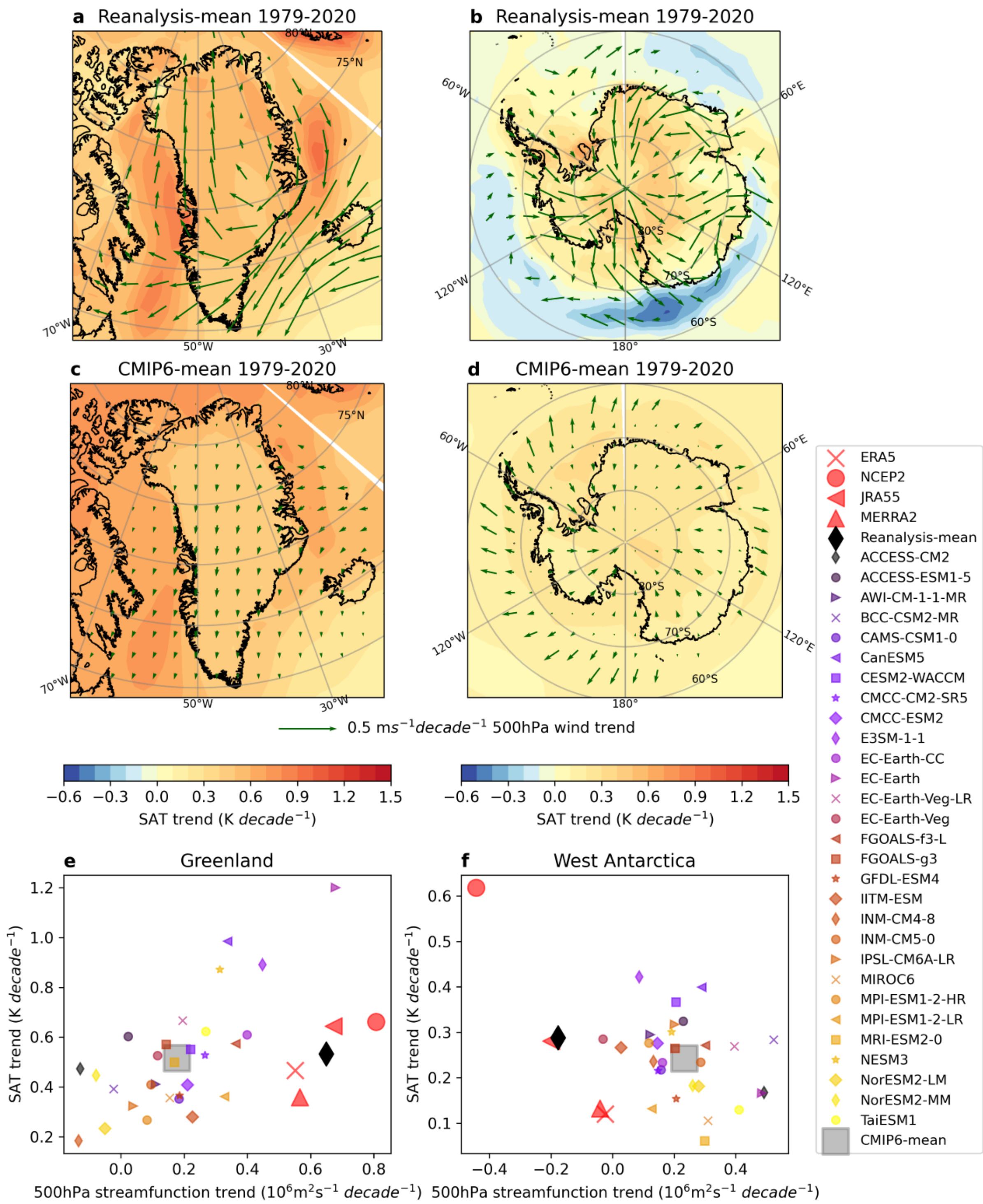

Figure 5. **Atmospheric circulation and associated surface temperature changes in meteorological reanalyses (ERA5, NCEP2, JRA55 and MERRA2) and CMIP6 global climate models. Annual mean surface air temperature (SAT) and wind trends over 1979-2020 in (a & b) the mean of four reanalyses (ERA5, NCEP2, JRA55 and MERRA2) and in (c & d) the mean of 29 CMIP6 models.** Shading: surface temperature trends; arrows: 500 hPa zonal/meridional

wind trends. Following ref. 244, SAT (y-axis) and 500hPa stream function (rotational component of winds, x-axis) trends in individual reanalyses and CMIP6 models (see legend) are also shown for both (e) Greenland (only land points) and (f) West Antarctica (60-90°S; 0-180°W; also only land points). This figure shows that winds are poorly represented by the GCMs for GrIS and that SAT and winds are poorly represented for the AIS.

Box 1 about MISI and MICI

Marine Ice Sheet Instability (MISI) is a self-enhancing process, triggered by external forcing (for example ocean warming), which results from the interactions between grounding lines, bed topography and ice dynamics. MISI is typically triggered by the thinning of a confined ice shelf, buttressing upstream flow, which leads to grounding line retreat. Once the grounding line is destabilised, it may continue to retreat in a self-enhancing fashion. How far the grounding line retreats depends on multiple factors, but the geometry of the bed topography is an important control on MISI: grounding lines are believed to be especially susceptible to such self-enhanced rapid retreat in regions of retrograde bed slopes. This irreversible process can be slowed down or stopped by several local factors, such as strong lateral shear stresses, or the presence of pinning points and morphological landforms[140]. These landforms can be pre-existing tectonic features or formed via the deposition of subglacial and ice proximal sediments[265-268]. Rapid uplift of the bed arising from glacio-isostatic adjustment can further shoal those features, potentially arresting rates of grounding line retreat (for example, refs. 269 and 270).

Marine Ice Cliff Instability (MICI) is a mechanism that is more hypothetical than MISI, but could also further amplify ice-sheet mass loss. This mechanism would be triggered by the collapse of ice shelves, exposing an ice cliff at the grounding line. If the ice cliff is tall enough, the stresses at the cliff may exceed the strength of ice, and the cliff may fail structurally, triggering repeated calving events[128]. Contrary to MISI, MICI does not require a retrograde bed slope to occur and could also happen on a flat or prograde terrain. Furthermore, the percolation of meltwater into newly-formed surface crevasses, alongside subsequent refreezing in situ, could further enlarge the crevasses and act to enhance MICI, leading to even faster rates of retreat[271]. Direct observations of cliff failure are, however, limited at present, making it difficult to assess whether MICI has ever occurred in the past. It is therefore still difficult to accurately parameterize the retreat of marine terminating glaciers that undergo cliff failure[93].